

An Iterative Algorithm for Sparse Recovery of Missing Image Samples Using a New Similarity Index

Amirhossein Javaheri, Hadi Zayyani, *Member, IEEE* and Farokh Marvasti, *Life Senior Member, IEEE*

Abstract—This paper investigates the problem of recovering missing samples using methods based on sparse representation adapted especially for image signals. Instead of ℓ_2 -norm or Mean Square Error (MSE), a new perceptual quality measure is used as the similarity criterion between the original and the reconstructed images. The proposed metric called Convex SIMilarity (CSIM) index is a modified version of the Structural SIMilarity (SSIM) index which despite its predecessor, is convex and uni-modal. We also propose an iterative sparse recovery method based on a constrained ℓ_1 -norm minimization problem involving CSIM as the fidelity criterion. This optimization problem which is adopted for missing sample recovery of images is efficiently solved via an algorithm based on Alternating Direction Method of Multipliers (ADMM). Simulation results show the performance of the new similarity index as well as the proposed algorithm for missing sample recovery of test images.

Index Terms—Missing Sample, Sparse Recovery, ADMM, Similarity Index, Image Inpainting.

I. INTRODUCTION

THE missing sample recovery problem arises in many applications in the literature of signal processing [1]–[3]. It is also known as inpainting in the context of audio and image processing. Audio inpainting is investigated in [4], while image inpainting is discussed in [5] and [6]. The missing sample recovery problem is also applied in the field of Wireless Sensor Network (WSN) [7] where some of the spatial samples are missed.

Among numerous algorithms for missing sample recovery and inpainting, some of them exploit the sparsity of the signals [2], [7], [8]. In this paper, we restrict ourselves to these sparse representation based algorithms. In this context, it is assumed that the signal is sparse in a domain such as Discrete Fourier Transform (DFT), Discrete Cosine Transform (DCT), Discrete Wavelet Transform (DWT) or any other predefined or learned complete or overcomplete dictionary. The sparsity of the signal on a dictionary based representation, means that the vector of coefficients of the signal in the transform domain has many zeros (or nearly zeros) and only a few of its elements are nonzero. Neglecting the insignificant (zero) coefficients, it is possible to reconstruct the signal with considerably low error. The sparsity of the signal gives us the ability to reconstruct it from very few random measurements far below the Nyquist

rate. This is well known as Compressed Sensing (CS) [9], [10], which has had many applications in the past decade [11]. The problem of reconstruction of the signal from a few random measurements is also known as sparse recovery. Many algorithms are proposed for sparse recovery of signals in different applications in audio and image processing.

In a missing sample recovery problem, some samples of the signal are missed due to physical impairment, unavailability of measurements, or distortion and disturbances. In such cases, it is shown that the corrupted samples would better be omitted throughout the reconstruction process [2]. Thus the discarded samples may be considered as missed. Even with these missing samples, the signal can still be reconstructed, given the sparsifying basis or dictionary and the corresponding sparse coefficients. Many algorithms and optimization problems are suggested to recover the sparse samples in this regard. The fundamental problem in a sparse recovery method is to maximize the sparsity which is principally stated in terms of the ℓ_0 -norm. There are a class of greedy algorithms for strictly sparse signal recovery based on ℓ_0 -norm minimization. These include Matching Pursuit (MP) [12], Orthogonal Matching Pursuit (OMP) [13], Regularized OMP (ROMP) [14], Compressive Sampling Matching Pursuit CoSaMP [15] and Generalized Matching Pursuit [16]. There are also iterative methods based on majorization minimization technique proposed for approximate ℓ_0 -norm minimization using surrogate functions. The Iterative Hard Thresholding (IHT) algorithm [17] is the first member of this class. There is also a modified version which uses adaptive thresholding named as Iterative Method with Adaptive Thresholding (IMAT) [18] with different variants including IMATI and IMATCS [19]. A recent improved version of this method called INPMAT is also proposed in [20]. Furthermore there is an approach for sparse approximation based on Smoothed- ℓ_0 (SL0) norm minimization presented in [21]. The ℓ_0 minimization algorithms are mostly used in cases where the signal has exactly sparse support and the sparsity is known. But in many practical situations the sparsity is unknown or the signal is not strictly sparse but instead compressible, meaning that most coefficients are negligible (despite being precisely zero) compared to the significant elements. A good and a common alternative is to use the ℓ_1 -norm as the nearest convex approximation of ℓ_0 -norm. This approach is called ℓ_1 minimization or the basis-pursuit method [22]. There are many algorithms presented for ℓ_1 -norm minimization including Iterative Soft Thresholding Algorithm (ISTA) [23] and the fast version FISTA [24],

Amirhossein Javaheri and Farokh Marvasti are both with Sharif University of Technology, Tehran, Iran. (email: javaheri_amirhossein@ee.sharif.edu; email: marvasti@sharif.edu).

H. Zayyani is with the Department of Electrical and computer Engineering, Qom University of Technology, Qom, Iran (e-mail: zayyani@qut.ac.ir).

ℓ_1 Least Squares (L1-LS) [25], Sparse Reconstruction by Separable Approximation (SpaRSA) [26], Primal and Dual Augmented Lagrangian Methods (PALM and DALM) [27], Iterative Bayesian Algorithm (IBA) [28], Sparse Bayesian Learning (SBL) [29] and Bayesian Compressed Sensing (BCS) [30]. There are also more general p -norm minimization based algorithms available for solving the sparse recovery problem in the literature [31]. For detailed survey on sparse recovery methods, one can refer to [32].

In this paper we propose an alternative ℓ_1 minimization method for sparse recovery of signals. Specifically we consider the sparse recovery of image patches with missing samples which has application in image inpainting and restoration. We introduce a criterion for measuring the similarity between two image signals which is called Convex SIMilarity (CSIM) Index. Although it is derived from the Structural SIMilarity (SSIM) index, the well-known perceptual quality assessment criterion [33], it has desirable mathematical features unlike its predecessor. In fact the advantage of the proposed index is its convexity and well-defined mathematical properties. These features result in simplified methods for solving the optimization problem involving this metric as the similarity index. In this paper we use this new index as fidelity criterion in our proposed optimization problem. Similar to [27], an iterative algorithm is presented for ℓ_1 minimization which uses Alternating Direction Method of Multipliers (ADMM) to solve the optimization problem. Simulation results show the efficiency of the proposed method called CSIM minimization via Augmented Lagrangian Method (CSIM-ALM) compared to some popular existing algorithms.

II. THE PROBLEM FORMULATION

The problem of recovering an image with samples missed at random, is equivalent to random sampling reconstruction of the signal. This problem is also addressed in the literature as block loss restoration due to error in the transmission channel [34], [35]. It is also known as image inpainting especially in applications where the sampling mask is known and the objective is to fill in the gaps or remove occlusion or specific objects from the image [6], [36]. Suppose $\mathbf{x} \in \mathbb{R}^N$ is the vectorized image signal and \mathbf{H} is the sampling matrix by which the pattern of sampling of the image signal is determined. In other words $\mathbf{H} \in \mathbb{R}^{m \times N}$ is obtained by eliminating $N - m$ rows of the identity \mathbf{I}_N matrix corresponding to the index of the missing samples. The observed image signal with missing samples, is also denoted by $\mathbf{y} \in \mathbb{R}^m$. There are many approaches for missing sample recovery of images or more specifically image inpainting including diffusion-based [37]–[39] and exemplar-based [41]–[43] methods. In this regard there are also a class of inpainting algorithms which use sparse representation for image restoration [5], [35]. If we assume that \mathbf{x} has approximately a sparse representation based on the atoms of a dictionary specified by the matrix \mathbf{D} , the regular optimization problem for sparse recovery of the missing samples is formulated as follows:

$$\min_{\mathbf{s}} \|\mathbf{s}\|_1 \quad s.t. \quad \begin{cases} \|\mathbf{H}\mathbf{x} - \mathbf{y}\|_2^2 \leq \epsilon_n \\ \mathbf{x} = \mathbf{D}\mathbf{s} \end{cases} \quad (1)$$

where \mathbf{s} denotes the sparse vector of representation coefficients and ϵ_n denotes the energy of the additive observation noise. The objective of the missing sample recovery problem is to reconstruct the original image \mathbf{x} based on observed remaining samples of the signal denoted by \mathbf{y} . This problem is also shown to be equivalent to:

$$\min_{\mathbf{s}, \mathbf{x}} \|\mathbf{H}\mathbf{x} - \mathbf{y}\|_2^2 + \alpha \|\mathbf{s}\|_1 \quad s.t. \quad \mathbf{x} = \mathbf{D}\mathbf{s} \quad (2)$$

In [5], [19], [44], [45] there are iterative algorithms proposed for recovery of missing samples exploiting the sparsity of representation based on redundant (over-complete) dictionaries. These algorithms mostly use global reconstruction methods in which the whole image is considered to have sparse approximation and the iterations of these algorithms are performed globally to obtain the entire reconstructed image at each step. This approach can further be improved extending the image sparsity to local viewpoint. In other words instead of global restoration an image can be divided into small patches and the sparsity is promoted using local transforms or dictionaries. In this approach the image is partitioned into a set of L overlapping patches of size $\sqrt{n} \times \sqrt{n}$ denoted by $\{\mathbf{x}_j\}_{j=1}^L$ and each patch $\mathbf{x}_j \in \mathbb{R}^n$ is assumed to have sparse coefficients on a local transform basis \mathbf{D} . Another improvement can also be achieved if we use adaptive dictionary instead of fixed \mathbf{D} . This dictionary can be learnt as in K-SVD [46] or be adopted to separate structures in an image called cartoon and texture as in MCA algorithm [44]. In [47] a localized or patch-based algorithm for missing sample recovery is presented which uses an adaptive dictionary learning method. In fact this algorithm tries to solve the optimization problem below:

$$\min_{\mathbf{s}, \mathbf{D}, \mathbf{x}} \|\mathbf{H}\mathbf{x} - \mathbf{y}\|_2^2 + \sum_{j=1}^L \alpha_j \|\mathbf{s}_j\|_1 + \lambda \sum_{j=1}^L \|\mathbf{H}_j(\mathbf{x}_j - \mathbf{D}\mathbf{s}_j)\|_2^2 \quad (3)$$

where \mathbf{x}_j and \mathbf{H}_j denote the j th patch of the reconstructed image and the mask respectively and \mathbf{s}_j denotes its corresponding sparse coefficients on the basis of \mathbf{D} . This problem is alternately solved comprising of two steps namely sparse coding and dictionary learning. In the sparse coding step, the dictionary is assumed fixed and the vector of sparse coefficients are obtained using sparse recovery methods like OMP. In the dictionary learning step an approach like K-SVD is used for adaptively learning a sparsifying dictionary based on existing sparse vectors. In this paper we propose an alternative method for sparse recovery of image signals which can be applied instead of OMP in the sparse coding step of an adaptive dictionary learning method for image inpainting. We also use perceptual metrics for visually enhanced reconstruction of the missing samples of the image as fidelity criterion instead of ℓ_2 norm. In the next section, we discuss more about the quality assessment metrics used for images.

III. QUALITY ASSESSMENT METRICS

A. A brief literature survey

There are different criteria for image quality or in other words similarity assessment. The most popular fidelity metric for measuring the similarity between two signals $\mathbf{x}, \mathbf{y} \in \mathbb{R}^n$

is MSE which is defined as $\text{MSE}(\mathbf{x}, \mathbf{y}) = \frac{1}{n} \|\mathbf{x} - \mathbf{y}\|_2^2$. This criterion is widely used to measure the quality performance of an estimator which is subsequently used to recover a signal with missing samples. This is apparently because MSE or equivalently ℓ_2 -norm is mathematically a well-defined function of the difference between the reference and the test signal. This function has desirable mathematical features such as convexity and differentiability which infers that it is simple and tractable to solve the optimization problem incurred by using this criterion as a penalty function. This optimization problem arises in any image recovery task such as denoising, deblurring and inpainting. Nevertheless there are cases in which the MSE criterion seems to be inefficient to accurately recover the original image signal especially in the presence of noise. One reason is that this fidelity metric is indifferent toward the error distribution, i.e., the statistics of the error signal. For instance consider two scenarios in which a signal is corrupted. In the first case the reference signal is perturbed by noise and in the second, a constant amplitude is added to the original image. Both corrupted images have the same MSE distortion metric with respect to the original image signal, while the noisy image is definitely more visually deteriorated. Thus there are a class of perceptual criteria introduced for measuring visual quality of images. The most popular perceptual metric is SSIM which is defined as [33]:

$$\text{SSIM}(\mathbf{x}, \mathbf{y}) = \left(\frac{2\mu_x\mu_y + C_1}{\mu_x^2 + \mu_y^2 + C_1} \right) \left(\frac{2\sigma_{x,y} + C_2}{\sigma_x^2 + \sigma_y^2 + C_2} \right) \quad (4)$$

where $C_1, C_2 > 0$ are constant and μ and σ denote the mean and the variance (cross-covariance) respectively. This function whose mathematical properties are discussed in [48], is non-convex and multi-modal implying that the problem of optimizing this criterion is hard to solve.

Another quality assessment metric is Feature SIMilarity (FSIM) index [49], which is proposed based on the fact that human visual system (HVS) perceives the image quality mainly based on its low-level features. In [49], phase congruency (PC) and gradient magnitude (GM) are considered as primary and secondary features used in characterizing the image local quality. Moreover, there are other fidelity metrics in the literature such as an information theoretic index called Visual Information Fidelity (VIF) [50], Multi-Scale SSIM (MS-SSIM) [51], Dynamic Range Independent Measure (DRIM) [52], and Tone-Mapped Quality Index (TMQI) [53]. For further investigation on subjective and objective quality assessment criteria, one can refer to [54].

B. The proposed performance metric

As mentioned earlier, SSIM function is non-convex and multi-modal which results in hard optimization problems to solve. Hence, in this paper, we define a simplified criterion derived from the numerator and the denominator terms appearing in (4). The proposed index named CSIM, is defined as follows:

$$\text{CSIM}(\mathbf{x}, \mathbf{y}) = k_1(\mu_x^2 + \mu_y^2 - 2\mu_x\mu_y) + k_2(\sigma_x^2 + \sigma_y^2 - 2\sigma_{x,y}) \quad (5)$$

where k_1 and k_2 are positive constants. Let us assume that $k_1 \ll k_2$; this is to ensure biased sensitivity toward random

disturbances or noise compared to uniform change. In fact unlike MSE, the new criterion has noise-sensitive variation. In other words a constant change in the brightness level of the image does not alter this criterion as much as the case of noisy disturbance does. This is logically because constant change in the amplitude only affects the signal mean value. It does not change variance/ cross-covariance. Thus as far as $k_1 \ll k_2$ the function CSIM is only slightly influenced by mere brightness level change. The metric above also benefits some feasible mathematical features. For example it is a convex and a positive-definite function of \mathbf{x} or \mathbf{y} . In the following we state two remarks in this correspondence.

Remark 1. The fidelity criterion defined by the function in (5), is positive-definite.

Proof. Suppose $\mathbf{x}, \mathbf{y} \in \mathbb{R}^n$, then

$$\begin{aligned} \sigma_x^2 &= \frac{1}{n-1} \|\mathbf{x} - \boldsymbol{\mu}_x\|_2^2, \quad \boldsymbol{\mu}_x = \mu_x \mathbf{1}_n \\ \sigma_{x,y} &= \frac{1}{n-1} (\mathbf{x} - \boldsymbol{\mu}_x)^T (\mathbf{y} - \boldsymbol{\mu}_y) \end{aligned} \quad (6)$$

Note that we have used the unbiased estimate for variance and covariance. Therefore

$$\begin{aligned} \sigma_x^2 + \sigma_y^2 - 2\sigma_{x,y} &= \frac{1}{n-1} \|\mathbf{x} - \boldsymbol{\mu}_x\|_2^2 + \frac{1}{n-1} \|\mathbf{y} - \boldsymbol{\mu}_y\|_2^2 \\ &\quad - \frac{2}{n-1} (\mathbf{x} - \boldsymbol{\mu}_x)^T (\mathbf{y} - \boldsymbol{\mu}_y) \\ &= \frac{1}{n-1} \|(\mathbf{x} - \boldsymbol{\mu}_x) - (\mathbf{y} - \boldsymbol{\mu}_y)\|_2^2 \end{aligned} \quad (7)$$

where the equality is satisfied if and only if $(\mathbf{x} - \boldsymbol{\mu}_x) = (\mathbf{y} - \boldsymbol{\mu}_y)$. On the other hand

$$\mu_x^2 + \mu_y^2 - 2\mu_x\mu_y = (\mu_x - \mu_y)^2 \quad (8)$$

Hence, if we define the error as the difference between these two signals, i.e., $\mathbf{e} = \mathbf{x} - \mathbf{y}$, the function in (5) may be simplified as:

$$\begin{aligned} \text{CSIM}(\mathbf{x}, \mathbf{y}) &= \text{CSIM}(\mathbf{x} - \mathbf{y}) \\ &= \text{CSIM}(\mathbf{e}) = k_1\mu_e^2 + \frac{k_2}{n-1} \|\mathbf{e} - \mu_e \mathbf{1}_n\|_2^2 \end{aligned} \quad (9)$$

where $\mathbf{1}_n = (1, \dots, 1) \in \mathbb{R}^n$. Now since $k_1, k_2 > 0$, the function above is obviously positive-definite and equals zero if and only if $\mathbf{e} = \mathbf{0}$ or equivalently $\mathbf{x} = \mathbf{y}$ \square

Remark 2. The fidelity criterion defined by the function in (5) is convex with respect to \mathbf{x} or \mathbf{y} .

Proof. One can rewrite equation (5) algebraically using the simplification as follows:

$$\begin{aligned} f(\mathbf{e}) &= \text{CSIM}(\mathbf{e}) \\ &= k_1\mu_e^T \mu_e + \frac{k_2}{n-1} (\mathbf{e} - \mu_e \mathbf{1}_n)^T (\mathbf{e} - \mu_e \mathbf{1}_n) \\ &= \frac{k_1}{n^2} \mathbf{e}^T \mathbf{1}_n \mathbf{1}_n^T \mathbf{e} + \frac{k_2}{n-1} \mathbf{e}^T \mathbf{M}^T \mathbf{M} \mathbf{e} \\ &= \mathbf{e}^T \left(\frac{k_1}{n^2} \mathbf{1}_n \mathbf{1}_n^T + \frac{k_2}{n-1} \mathbf{M} \right) \mathbf{e} \end{aligned} \quad (10)$$

where $\mathbf{M} = (\mathbf{I}_n - \frac{1}{n}\mathbf{1}_n\mathbf{1}_n^T)$ and \mathbf{I}_n is the identity matrix. Therefore

$$\text{CSIM}(\mathbf{e}) = \mathbf{e}^T \mathbf{W} \mathbf{e} \quad (11)$$

and $\mathbf{W} \in \mathbb{R}^{n \times n}$ is

$$\mathbf{W} = \frac{k_2}{n-1} \mathbf{I}_n + \left(\frac{k_1}{n^2} - \frac{k_2}{n(n-1)} \right) \mathbf{1}_n \mathbf{1}_n^T \quad (12)$$

Now since f is a continuous and twice differentiable function of \mathbf{e} , to prove its convexity, it is sufficient to show that the Hessian of f or equivalently \mathbf{W} is positive-semidefinite. Once the convexity of f with respect to $\mathbf{e} = \mathbf{x} - \mathbf{y}$ has been affirmed, it will also be concluded that CSIM is convex with respect to \mathbf{x} or \mathbf{y} . \square

Now the objective is to compute the eigenvalues of \mathbf{W} to approve the convexity of CSIM, but beforehand we need to express the following lemma:

Lemma 1. Let $\mathbf{Q} = \mathbf{P} + \gamma \mathbf{I}_n$ where $\mathbf{P}, \mathbf{Q} \in \mathbb{R}^{n \times n}$. If the eigenvalues of \mathbf{P} are given as $\lambda_{\mathbf{P}_1} \leq \lambda_{\mathbf{P}_2} \leq \dots \leq \lambda_{\mathbf{P}_n}$, then the eigenvalues of \mathbf{Q} will be obtained using the following equation:

$$\lambda_{\mathbf{Q}_i} = \gamma + \lambda_{\mathbf{P}_i} \quad (13)$$

Proof. The proof is trivial exploiting the definition of the eigenvalues and eigenvectors of \mathbf{Q} . \square

Now back to our discussion, let us assume $\mathbf{P} = \left(\frac{k_1}{n^2} - \frac{k_2}{n(n-1)} \right) \mathbf{1}_n \mathbf{1}_n^T$, $\mathbf{Q} = \mathbf{W}$ and $\gamma = \frac{k_2}{n-1}$. Now using lemma 1 we can obtain the eigenvalues of \mathbf{W} . But firstly we need to compute the eigenvalues of \mathbf{P} . Since \mathbf{P} is symmetric and has a maximum rank of one, it can be concluded that there is only a single non-zero eigenvalue denoted by $\lambda_{\mathbf{P}_n}$ which satisfies:

$$\mathbf{P} \mathbf{v}_{\mathbf{P}_n} = \left(\frac{k_1}{n^2} - \frac{k_2}{n(n-1)} \right) \mathbf{1}_n \mathbf{1}_n^T \mathbf{v}_{\mathbf{P}_n} = \lambda_{\mathbf{P}_n} \mathbf{v}_{\mathbf{P}_n} \quad (14)$$

and all the remaining eigenvalues $\lambda_{\mathbf{P}_i}$, $1 \leq i \leq n-1$ are zero. Now if we set $\mathbf{v}_{\mathbf{P}_n} = \mathbf{1}_n$, then $\lambda_{\mathbf{P}_n}$ is given by:

$$\lambda_{\mathbf{P}_n} = \left(\frac{k_1}{n^2} - \frac{k_2}{n(n-1)} \right) \mathbf{1}_n^T \mathbf{1}_n = \frac{k_1}{n} - \frac{k_2}{n-1} \quad (15)$$

So:

$$\lambda_{\mathbf{P}_i} = \begin{cases} 0, & i < n \\ \frac{k_1}{n} - \frac{k_2}{n-1}, & i = n \end{cases} \quad (16)$$

Consequently the eigenvalues of the kernel matrix \mathbf{Q} are obtained by:

$$\lambda_{\mathbf{W}_i} = \lambda_{\mathbf{P}_i} + \frac{k_2}{n-1} = \begin{cases} \frac{k_2}{n-1}, & i < n \\ \frac{k_1}{n}, & i = n \end{cases} \quad (17)$$

Therefore the primary assumption $k_1 \ll k_2$ is not a necessary condition to approve the convexity of CSIM and it only suffices for k_1 and k_2 to be non-negative.

Now the problem is how to find k_1 and k_2 so that the proposed criterion has utmost sensitivity to random perturbation compared to uniform change. Assume a random binary signal

with i.i.d. elements taking $\{a, -a\}$ with equal probability, is added to the reference signal \mathbf{x} , i.e.:

$$\mathbf{y}_1 = \mathbf{x} + \mathbf{e}_1, \quad C_{\mathbf{e}_1} = \mathbb{E}[\mathbf{e}_1 \mathbf{e}_1^T] = a^2 \mathbf{I}_n \quad (18)$$

Consider another scenario in which \mathbf{x} is added by a deterministic signal \mathbf{e}_2 with constant amplitude a , i.e., $\mathbf{y}_2 = \mathbf{x} + a \mathbf{1}_n$. Now we define the ratio of sensitivity as:

$$\rho = \frac{\mathbb{E}[\text{CSIM}(\mathbf{x}, \mathbf{y}_1)]}{\mathbb{E}[\text{CSIM}(\mathbf{x}, \mathbf{y}_2)]} = \frac{\mathbb{E}[\text{CSIM}(\mathbf{e}_1)]}{\mathbb{E}[\text{CSIM}(\mathbf{e}_2)]} = \frac{\mathbb{E}[\mathbf{e}_1^T \mathbf{W} \mathbf{e}_1]}{\mathbf{e}_2^T \mathbf{W} \mathbf{e}_2} \quad (19)$$

Remark 3. The sensitivity ratio is equal to $\rho = \frac{\sum_i w_{i,i}}{\sum_i \sum_j w_{i,j}}$.

Proof. Let $\mathbf{e}_2 = a \mathbf{1}_n$ and $C_{\mathbf{e}_1} = a^2 \mathbf{I}_n$. Since for a scalar variable c , we have $c = \text{trace}(c)$, we may write:

$$\begin{aligned} \mathbb{E}[\mathbf{e}_1^T \mathbf{W} \mathbf{e}_1] &= \text{trace}(\mathbb{E}[\mathbf{e}_1^T \mathbf{W} \mathbf{e}_1]) = \mathbb{E}[\text{trace}(\mathbf{e}_1^T \mathbf{W} \mathbf{e}_1)] \\ &= \text{trace}(\mathbb{E}[\mathbf{e}_1 \mathbf{e}_1^T] \mathbf{W}) = a^2 \text{trace}(\mathbf{W}) \end{aligned} \quad (20)$$

Similarly, we have:

$$\mathbf{e}_2^T \mathbf{W} \mathbf{e}_2 = a^2 \mathbf{1}_n^T \mathbf{W} \mathbf{1}_n = a^2 \sum_i \sum_j w_{i,j} \quad (21)$$

\square

Now for \mathbf{W} defined in (13), the sensitivity ratio would be simplified to:

$$\rho = \frac{\frac{k_2}{n-1} + \left(\frac{k_1}{n^2} - \frac{k_2}{n(n-1)} \right)}{\frac{k_2}{n-1} + \left(\frac{k_1}{n} - \frac{k_2}{n-1} \right)} = \frac{k_2}{k_1} + \frac{1}{n} \quad (22)$$

This relation states that the greater the ratio k_2/k_1 is, the more sensitive the proposed CSIM index will be toward noise. But there are other conditions which impose constraints on the eigenvalues of \mathbf{W} and accordingly the values of k_1 and k_2 . One is the condition number. Consider the optimization problem below:

$$\min_{\mathbf{s}} \text{CSIM}(\mathbf{D}\mathbf{s}, \mathbf{y}) = (\mathbf{D}\mathbf{s} - \mathbf{y})^T \mathbf{W} (\mathbf{D}\mathbf{s} - \mathbf{y}) \quad (23)$$

Since \mathbf{W} is Hermitian and positive-definite, it is diagonalizable and thus, $\mathbf{W}^{1/2}$ exists and is as follows:

$$\mathbf{W}^{1/2} = (\beta_1 \mathbf{I}_n + \beta_2 \mathbf{1}_n \mathbf{1}_n^T) \quad (24)$$

where β_1 and β_2 are obtained by:

$$\begin{aligned} \beta_1 &= \sqrt{\frac{k_2}{n-1}} \\ \beta_2 &= \frac{1}{n} \left(\sqrt{\frac{k_1}{n}} - \sqrt{\frac{k_2}{n-1}} \right) \end{aligned} \quad (25)$$

Hence, we can rewrite (23) as:

$$\min_{\mathbf{s}} (\mathbf{D}\mathbf{s} - \mathbf{y})^T \mathbf{W}^{\frac{1}{2}} \mathbf{W}^{\frac{1}{2}} (\mathbf{D}\mathbf{s} - \mathbf{y}) = \|\mathbf{D}'\mathbf{s} - \mathbf{y}'\|_2^2 \quad (26)$$

where $\mathbf{D}' = \mathbf{W}^{1/2} \mathbf{D}$ and $\mathbf{y}' = \mathbf{W}^{1/2} \mathbf{y}$. The solution to (26) is obtained as $\mathbf{D}'^\dagger \mathbf{y}' = (\mathbf{D}'^T \mathbf{W} \mathbf{D}')^{-1} \mathbf{D}'^T \mathbf{W} \mathbf{y}$. For (26) to have a robust (reliable) solution, the matrix \mathbf{W} must not be ill-conditioned. Now assuming $k_2 > k_1$, using (17), we can write:

$$\kappa(\mathbf{W}) = \frac{\lambda_{\max}(\mathbf{W})}{\lambda_{\min}(\mathbf{W})} = \left(\frac{n}{n-1} \right) \frac{k_2}{k_1} \leq \kappa_{\max} \quad (27)$$

where $\kappa(\mathbf{W})$ denotes the condition number of \mathbf{W} and κ_{\max} denotes the maximum value of condition number permitted. Another constraint is imposed by adding ℓ_1 -norm penalty to the cost function in (26), i.e.:

$$\min_{\mathbf{s}} \|\mathbf{D}'\mathbf{s} - \mathbf{y}'\|_2^2 + \alpha \|\mathbf{s}\|_1 \quad (28)$$

This cost function can be iteratively optimized using ISTA [23], and the estimated solution at iteration t is obtained by:

$$\mathbf{s}^{(t)} = S_{\frac{\alpha}{2}} \left(\mathbf{s}^{(t-1)} + \mathbf{D}'^T (\mathbf{y}' - \mathbf{D}'\mathbf{s}^{(t-1)}) \right) \quad (29)$$

where S denotes the soft-thresholding operator [55]. A sufficient condition to insure (29) converges to the solution of (28) and is its unique minimizer, is that $\text{Null}(\mathbf{D}') = \{\mathbf{0}\}$ and the spectral norm of \mathbf{D}' should be less than unity [23]. Since $\mathbf{W}^{\frac{1}{2}}$ is invertible, the first condition is satisfied as far as $\text{Null}(\mathbf{D}') = \{\mathbf{0}\}$. Therefore:

$$\|\mathbf{D}'\|_2 = \|\mathbf{W}^{\frac{1}{2}}\mathbf{D}\|_2 \leq 1 \quad (30)$$

Now since $\|\mathbf{W}^{\frac{1}{2}}\mathbf{D}\|_2 \leq \|\mathbf{W}^{\frac{1}{2}}\|_2 \|\mathbf{D}\|_2$, if we assume $\|\mathbf{D}\|_2 \leq \sigma_0$, a sufficient condition could be expressed as:

$$\|\mathbf{W}^{\frac{1}{2}}\|_2 = \sigma_{\max}(\mathbf{W}^{\frac{1}{2}}) = \sqrt{\lambda_{\max}(\mathbf{W})} = \sqrt{\frac{k_2}{n-1}} \leq \frac{1}{\sigma_0} \quad (31)$$

Since a larger value of $\|\mathbf{D}'\|_2$ guarantees lower $\|\mathbf{I}_n - \mathbf{D}'^T\mathbf{D}\|_2$ and consequently faster rate of convergence [56], to gain maximum ρ , we choose:

$$k_2 = \frac{n-1}{\sigma_0^2}, \quad k_1 = \frac{n}{\sigma_0^2 \kappa_{\max}} \quad (32)$$

In the next sections we assume $\sigma_0 = 1$ and let $\kappa_{\max} = 5$.

IV. THE PROPOSED SPARSE RECOVERY ALGORITHM FOR MISSING SAMPLE RECOVERY

As discussed earlier in section II most of the algorithms use ℓ_2 norm as fidelity criterion for image reconstruction. But there are also inpainting methods based on local sparse representation which use perceptual image quality assessment metrics for recovery of the missing samples. In [57] an exemplar-based method for image completion is proposed which uses adaptive dictionary learning for sparse recovery of local image patches. In this algorithm, for each candidate patch the optimization problem below is solved in the sparse coding step:

$$\max_{\mathbf{x}, \mathbf{s}} \text{SSIM}(\mathbf{x}, \mathbf{D}\mathbf{s}) \quad s.t. \quad \begin{cases} \mathbf{H}\mathbf{x} = \mathbf{y} \\ \|\mathbf{s}\|_0 \leq T \end{cases} \quad (33)$$

where for simplicity we have omitted the index of the patch \mathbf{x} and its corresponding sparse representation vector \mathbf{s} . This optimization problem is iteratively solved using a matching pursuit approach, i.e., in each step the support of the sparse vector is retrieved and the coefficients are subsequently obtained solving unconstrained (33). This problem is non-convex and thus solved using time-consuming linear search methods. Here we propose to use CSIM instead of SSIM in the optimization problem. Hence, to solve the missing sample recovery problem defined in (1), we incorporate our proposed

perceptual metric for reconstruction of the image samples. We do this by adding another constraint to this problem confining the CSIM of $\mathbf{H}\mathbf{x}$ and \mathbf{y} to be less than a predefined value, i.e. $\text{CSIM}(\mathbf{H}\mathbf{x}, \mathbf{y}) \leq \theta$. This is to insure reconstruction quality in terms of our proposed fidelity criterion. Besides consider we have an estimate of the missed samples of \mathbf{x} which is denoted by $\mathbf{y}_c = \mathbf{H}_c\mathbf{x}$ where \mathbf{H}_c specifies the complement set of the sampling indices of \mathbf{H} . This estimate may be obtained by interpolating the signal \mathbf{x} (with missed samples) or in an exemplar inpainting method, it is actually the nearest exemplar of the corrupted patch of the image. Hence, the constraint $\text{CSIM}(\mathbf{H}_c\mathbf{x}, \mathbf{y}_c) \leq \theta$ imposes some sort of fidelity criterion over the indices of the signal with unknown sample values. We will talk about this later in the method we propose for image inpainting. For now simply let $\mathbf{H}_c = \mathbf{H}$ and $\mathbf{y}_c = \mathbf{y}$. Now using Lagrange multipliers theorem, the new problem is equivalent to:

$$\min_{\mathbf{x}, \mathbf{s}} \frac{1}{2} \|\mathbf{H}\mathbf{x} - \mathbf{y}\|_2^2 + \alpha_1 \|\mathbf{s}\|_1 + \alpha_2 \text{CSIM}(\mathbf{H}\mathbf{x}, \mathbf{y}) \quad s.t. \quad \mathbf{x} = \mathbf{D}\mathbf{s} \quad (34)$$

where α_1 and α_2 are chosen such that Karush-Kuhn-Tucker (KKT) conditions are satisfied [58]. Note that since CSIM is convex and uni-modal finding the local minima of (34) is sufficient to attain its global optimum. Now introducing an auxiliary variable defined as $\mathbf{z} = \mathbf{H}\mathbf{x}$ the optimization problem (19) would change to:

$$\min_{\mathbf{x}, \mathbf{s}, \mathbf{z}} \frac{1}{2} \|\mathbf{H}\mathbf{x} - \mathbf{y}\|_2^2 + \alpha_1 \|\mathbf{s}\|_1 + \alpha_2 \text{CSIM}(\mathbf{z}, \mathbf{y}) \quad s.t. \quad \begin{cases} \mathbf{x} = \mathbf{D}\mathbf{s} \\ \mathbf{z} = \mathbf{H}\mathbf{x} \end{cases} \quad (35)$$

The auxiliary variable is used to separate the optimization problem involving CSIM as the fidelity index. Since the CSIM function is convex, it is guaranteed use the Alternating Direction Method of Multipliers (ADMM) [59] to solve (20). Hence the final cost function to be optimized is the augmented Lagrangian function:

$$\begin{aligned} \min_{\mathbf{x}, \mathbf{s}, \mathbf{z}} \mathcal{L}(\mathbf{x}, \mathbf{s}, \mathbf{z}) = & \frac{1}{2} \|\mathbf{H}\mathbf{x} - \mathbf{y}\|_2^2 + \alpha_1 \|\mathbf{s}\|_1 + \alpha_2 \text{CSIM}(\mathbf{z}, \mathbf{y}) \\ & + \mu_1^T (\mathbf{x} - \mathbf{D}\mathbf{s}) + \frac{\sigma_1}{2} \|\mathbf{x} - \mathbf{D}\mathbf{s}\|_2^2 \\ & + \mu_2^T (\mathbf{z} - \mathbf{H}\mathbf{x}) + \frac{\sigma_2}{2} \|\mathbf{z} - \mathbf{H}\mathbf{x}\|_2^2 \end{aligned} \quad (36)$$

The ADMM alternatively minimizes (36) with respect to each variable while assuming the other variables fixed. Hence at each iteration of the ADMM, the problem (36) is split into three sub-problems as follows:

A. \mathbf{x} sub-problem:

The augmented Lagrangian cost function with respect to \mathbf{x} is a quadratic function. Hence, the optimization sub-problem associating with \mathbf{x} at t -th iteration of the ADMM is:

$$\begin{aligned} \mathbf{x}^{(t+1)} = & \underset{\mathbf{x}}{\text{argmin}} \mathcal{L}(\mathbf{x}, \mathbf{s}^{(t)}, \mathbf{z}^{(t)}) \\ = & \underset{\mathbf{x}}{\text{argmin}} \mathcal{L}(\mathbf{x}) = \mathbf{x}^T \mathbf{Q}\mathbf{x} + \mathbf{b}^{(t)T} \mathbf{x} \end{aligned} \quad (37)$$

where $\mathbf{Q} = \frac{1+\sigma_2}{2}\mathbf{H}^T\mathbf{H} + \frac{\sigma_1}{2}\mathbf{I}$ and $\mathbf{b}^{(t)} = -\mathbf{H}^T\mathbf{y} + \boldsymbol{\mu}_1^{(t)} - \sigma_1\mathbf{D}\mathbf{s}^{(t)} - \mathbf{H}^T\boldsymbol{\mu}_2^{(t)} - \sigma_2\mathbf{H}^T\mathbf{z}^{(t)}$. The solution to this problem is simply obtained by differentiation and it is:

$$\mathbf{x}^{(t+1)} = -\frac{1}{2}\mathbf{Q}^{-1}\mathbf{b}^{(t)} = -\frac{1}{2}\left(\frac{\sigma_1}{2}\mathbf{I} + \frac{1+\sigma_2}{2}\mathbf{H}^T\mathbf{H}\right)^{-1}\mathbf{b}^{(t)} \quad (38)$$

Now since $\mathbf{H}\mathbf{H}^T$ is equivalent to consecutively projecting the extracted samples back to the initial higher dimensional space and repeating the sampling process, $\mathbf{H}\mathbf{H}^T = \mathbf{I}$. Hence, using Sherman-Morrison-Woodbury lemma [60], the solution to (38) would be simplified to:

$$\mathbf{x}^{(t+1)} = -\frac{1}{\sigma_1}\left(\mathbf{I} - \frac{1}{1+\tilde{\mu}}\mathbf{H}^T\mathbf{H}\right)\mathbf{b}^{(t)}, \quad \tilde{\mu} = \frac{\sigma_1}{1+\sigma_2} \quad (39)$$

B. s sub-problem:

The optimization sub-problem associating with \mathbf{s} is:

$$\begin{aligned} \mathbf{s}^{(t+1)} &= \underset{\mathbf{s}}{\operatorname{argmin}} \mathcal{L}(\mathbf{x}^{(t+1)}, \mathbf{s}, \mathbf{z}^{(t)}) \\ &= \underset{\mathbf{s}}{\operatorname{argmin}} \mathcal{L}(\mathbf{s}) = \frac{1}{2}\|\mathbf{x}^{(t+1)} - \mathbf{D}\mathbf{s}\|_2^2 + \frac{\alpha_1}{\sigma_1}\|\mathbf{s}\|_1 \\ &\quad + \frac{1}{\sigma_1}\boldsymbol{\mu}_1^{(t)T}(\mathbf{x}^{(t+1)} - \mathbf{D}\mathbf{s}) \end{aligned} \quad (40)$$

Assume $\|\mathbf{D}\|_2^2 \leq \lambda$, using the Majorization Minimization (MM) technique [61], we define a surrogate function similar to what is proposed in [23].

$$\begin{aligned} \mathcal{L}^S(\mathbf{s}, \mathbf{s}_0) &= \frac{1}{2}\|\mathbf{x}^{(t+1)} - \mathbf{D}\mathbf{s}\|_2^2 + \frac{1}{\sigma_1}\boldsymbol{\mu}_1^{(t)T}(\mathbf{x}^{(t+1)} - \mathbf{D}\mathbf{s}) \\ &\quad + \frac{\alpha_1}{\sigma_1}\|\mathbf{s}\|_1 + \frac{\lambda}{2}\|\mathbf{s}_0 - \mathbf{s}\|_2^2 - \frac{1}{2}\|\mathbf{D}\mathbf{s}_0 - \mathbf{D}\mathbf{s}\|_2^2 \end{aligned} \quad (41)$$

Since $\mathcal{L}^S(\mathbf{s}, \mathbf{s}_0) \geq \mathcal{L}(\mathbf{s})$, $\forall \mathbf{s}_0 \neq \mathbf{s}$ and $\mathcal{L}^S(\mathbf{s}, \mathbf{s}) = \mathcal{L}(\mathbf{s})$, optimizing (41) with respect to \mathbf{s} will reduce the initial cost function $\mathcal{L}(\mathbf{s})$. Hence by eliminating the unnecessary variables, the surrogate optimization problem is simplified to:

$$\begin{aligned} \min_{\mathbf{s}} \mathcal{L}^S(\mathbf{s}, \mathbf{s}_0) &= \min_{\mathbf{s}} -\mathbf{x}^{(t+1)T}\mathbf{D}\mathbf{s} + \frac{\alpha_1}{\sigma_1}\|\mathbf{s}\|_1 \\ &\quad - \frac{1}{\sigma_1}\boldsymbol{\mu}_1^{(t)T}\mathbf{D}\mathbf{s} - \lambda\mathbf{s}_0^T\mathbf{s} + \frac{\lambda}{2}\|\mathbf{s}\|_2^2 + \mathbf{s}_0^T\mathbf{D}^T\mathbf{D}\mathbf{s} \\ &= \min_{\mathbf{s}} \frac{\lambda}{2}\|\mathbf{s} - \mathbf{a}(\mathbf{s}_0)\|_2^2 + \frac{\alpha_1}{\sigma_1}\|\mathbf{s}\|_1 \end{aligned} \quad (42)$$

where $\mathbf{a}(\mathbf{s}_0) = \mathbf{s}_0 + \frac{1}{\lambda}\mathbf{D}^T(\mathbf{x}^{(t+1)} - \mathbf{D}\mathbf{s}_0 + \frac{1}{\sigma_1}\boldsymbol{\mu}_1^{(t)})$. Let us set $\mathbf{s}_0 = \mathbf{s}^{(t)}$, where t denotes the iteration number. Now the solution to (42) is obtained using the soft-thresholding operator and $\mathbf{s}^{(t)}$ is updated according to:

$$\mathbf{s}^{(t+1)} = S_{\frac{\alpha_1}{\lambda\sigma_1}}\left(\mathbf{s}^{(t)} + \frac{1}{\lambda}\mathbf{D}^T(\mathbf{x}^{(t+1)} - \mathbf{D}\mathbf{s}^{(t)} + \frac{1}{\sigma_1}\boldsymbol{\mu}_1^{(t)})\right) \quad (43)$$

Now since $\mathbf{s}^{(t+1)}$ is the minimizer of $\mathcal{L}^S(\mathbf{s}, \mathbf{s}^{(t)})$ we have:

$$\mathcal{L}(\mathbf{s}^{(t+1)}) \leq \mathcal{L}^S(\mathbf{s}^{(t+1)}, \mathbf{s}^{(t)}) \leq \mathcal{L}^S(\mathbf{s}^{(t)}, \mathbf{s}^{(t)}) = \mathcal{L}(\mathbf{s}^{(t)}) \quad (44)$$

where the first inequality comes from the fact that the surrogate function is the majorization of the original cost function. For this condition to be satisfied we use a backtracking procedure

to choose the appropriate value of λ . This method as proposed in [24], solves the optimization problem (42) and checks whether the solution \mathbf{s}^* satisfies $\mathcal{L}(\mathbf{s}^*) \leq \mathcal{L}^S(\mathbf{s}^*, \mathbf{s}^{(t)})$. If true the value of $\mathbf{s}^{(t+1)}$ is set to \mathbf{s}^* and if not, it multiplies the value of λ by a constant $\beta > 1$. Hence it is an adaptive approach to specify the threshold $\frac{\alpha_1}{\lambda\sigma_1}$.

C. z sub-problem

The sub-problem associating with \mathbf{z} is as follows:

$$\begin{aligned} \mathbf{z}^{(t+1)} &= \underset{\mathbf{z}}{\operatorname{argmin}} \mathcal{L}(\mathbf{x}^{(t+1)}, \mathbf{s}^{(t+1)}, \mathbf{z}) \\ &= \underset{\mathbf{z}}{\operatorname{argmin}} \mathcal{L}(\mathbf{z}) = \alpha_2\text{CSIM}(\mathbf{z}, \mathbf{y}) + \boldsymbol{\mu}_2^{(t)T}(\mathbf{z} - \mathbf{H}\mathbf{x}^{(t+1)}) \\ &\quad + \frac{\sigma_2}{2}\|\mathbf{z} - \mathbf{H}\mathbf{x}^{(t+1)}\|_2^2 \end{aligned} \quad (45)$$

Now substituting CSIM from (5), the resulting cost function will be in the quadratic form below:

$$\mathbf{z}^{(t+1)} = \underset{\mathbf{z}}{\operatorname{argmin}} \mathbf{z}^T\mathbf{K}\mathbf{z} + \mathbf{c}^{(t)T}\mathbf{z} \quad (46)$$



Fig. 2. The set of gray-scale images from which 8×8 patches are extracted for simulations in this paper. From top to bottom and left to right: Barbara, Lena, Cameraman, Clown, Couple, House, Orca and Peppers

Algorithm 1 CSIM-ALM algorithm

To solve the optimization problem (36)

set $\sigma_1, \sigma_2 > 0$, $\beta > 1$, $\lambda = \alpha_2 = 1$, $\eta < 1$, $\alpha_{\min} \ll 1$, $k_1, k_2 > 0$

initialize $\boldsymbol{\mu}_1^{(0)} = \boldsymbol{\mu}_2^{(0)} = \mathbf{0}$, $\mathbf{z}^{(0)} = \mathbf{H}\mathbf{y}$, $\mathbf{s}^{(0)} = \mathbf{s}^{*(-1)} = \mathbf{0}$, $\gamma^{(0)} = 1$, $t = 0$.

- 1: **repeat**
- 2: Update $\mathbf{r}^{(t)} = \mathbf{y} - \mathbf{H}\mathbf{D}\mathbf{s}^{(t)}$
- 3: Update $\alpha_1 = \max\{\eta\|\mathbf{D}^T\mathbf{H}^T\mathbf{r}^{(t)}\|_\infty, \alpha_{\min}\}$
- 4: Update $\mathbf{b}^{(t)}$ and $\mathbf{x}^{(t+1)}$ using (37) and (39)
- 5: **repeat**
- 6: Obtain $\mathbf{s}^{*(t)}$ by solving (42) assuming $\mathbf{s}_0 = \mathbf{s}^{(t)}$
- 7: Set $\lambda = \lambda \times \beta$,
- 8: **until** $\mathcal{L}(\mathbf{s}^{*(t)}) \leq \mathcal{L}^S(\mathbf{s}^{*(t)}, \mathbf{s}^{(t)})$
- 9: Update $\gamma^{(t+1)} = \frac{1 + \sqrt{1 + (2\gamma^{(t)})^2}}{2}$
- 10: Update $\mathbf{s}^{(t+1)} = \mathbf{s}^{*(t)} + \left(\frac{\gamma^{(t)} - 1}{\gamma^{(t+1)}}\right)(\mathbf{s}^{*(t)} - \mathbf{s}^{*(t-1)})$
- 11: Update $\mathbf{z}^{(t+1)}$ by solving (46) using \mathbf{K}^{-1} as in (47)
- 12: Update $\boldsymbol{\mu}_1^{(t+1)}$ and $\boldsymbol{\mu}_2^{(t+1)}$ according to (48)
- 13: $t \leftarrow t + 1$
- 14: **until** A stopping criterion is reached

TABLE I
PERFORMANCE COMPARISON OF THE FIR DENOISING FILTERS OF ORDER m FOR SIMULATIONS IN PART V-A.1, (SNR=1dB)

		$m = 6$			$m = 12$		
		MSE Filter	CSIM Filter	SSIM Filter	MSE Filter	CSIM Filter	SSIM Filter
Peppers	PSNR (dB)	22.02624	19.59074	18.74218	23.01379	20.51426	18.92838
	SSIM	0.437667	0.463604	0.445002	0.488934	0.513346	0.50831
	FSIM	0.725322	0.752717	0.733245	0.753915	0.774345	0.763619
	Time (s)	7.703125	8.671875	232.375	11.32813	21.45313	210.5
Lena	PSNR (dB)	23.47825	21.01571	19.62036	24.47371	21.92508	19.82099
	SSIM	0.497242	0.520295	0.506187	0.54762	0.567756	0.571409
	FSIM	0.763082	0.790042	0.777688	0.787491	0.807698	0.807059
	Time (s)	6.984375	8.40625	201.5781	10.48438	15.82813	206.9375
Barbara	PSNR (dB)	22.19703	20.21621	18.89702	23.18561	21.16635	19.115
	SSIM	0.517242	0.537474	0.529405	0.577095	0.593189	0.591923
	FSIM	0.749932	0.773378	0.75956	0.775784	0.794461	0.784306
	Time (s)	7.46875	7.984375	228.375	12.48438	15.54688	236.7344
House	PSNR (dB)	22.05487	19.64165	18.80577	23.03948	20.47174	19.07671
	SSIM	0.387762	0.396543	0.385529	0.439848	0.455067	0.447596
	FSIM	0.69685	0.72486	0.695154	0.723184	0.744779	0.72871
	Time (s)	8	9.78125	232.0625	10.07813	15.40625	238.5
Cameraman	PSNR (dB)	21.99298	19.3455	18.53909	23.0564	20.35864	18.81843
	SSIM	0.463839	0.488692	0.475355	0.524988	0.550085	0.543624
	FSIM	0.765743	0.793235	0.782742	0.790887	0.81209	0.809912
	Time (s)	7.28125	8.078125	233.6094	9.796875	15.54688	239.6875
Couple	PSNR (dB)	23.09378	21.41167	18.93118	23.93885	22.19459	19.13656
	SSIM	0.531812	0.542148	0.544879	0.578546	0.589889	0.611208
	FSIM	0.806133	0.816203	0.810392	0.826742	0.831216	0.834012
	Time (s)	7.578125	10.35938	232.1719	9.859375	14.04688	236.625



Fig. 1. Noisy images Peppers (1a) and Lena (1e) (SNR=1dB) denoised with FIR filters of order $m = 6$, For PSNR, SSIM and FSIM values refer to Table I.

where $\mathbf{K} = \frac{\sigma_2}{2}\mathbf{I} + \alpha_2\mathbf{W}$ and $\mathbf{c}^{(t)} = \boldsymbol{\mu}_2^{(t)} - \sigma_2\mathbf{H}\mathbf{x}^{(t+1)} - 2\alpha_2\mathbf{W}^T\mathbf{y}$. The solution to (46) is $\mathbf{z}^{(t+1)} = \mathbf{K}^{-1}\mathbf{c}^{(t)}$. To calculate the inverse of \mathbf{K} we use the matrix inverse lemma:

$$\mathbf{K} = \theta_1\mathbf{I}_n + \theta_2\mathbf{1}_n\mathbf{1}_n^T, \quad \mathbf{K}^{-1} = \frac{1}{\theta_1} \left(\mathbf{I}_n - \frac{\theta_2}{\theta_1 + n\theta_2} \mathbf{1}_n\mathbf{1}_n^T \right) \quad (47)$$

where $\theta_1 = \frac{\sigma_2}{2} + \alpha_2\frac{k_2}{n-1}$ and $\theta_2 = \alpha_2\left(\frac{k_1}{n^2} - \frac{k_2}{n(n-1)}\right)$.

D. Multipliers update

The final step of the ADMM is to update the Lagrangian multipliers associated with the equality constraints. Hence, we have:

$$\begin{aligned} \boldsymbol{\mu}_1^{(t+1)} &= \boldsymbol{\mu}_1^{(t)} + \sigma_1(\mathbf{x}^{(t+1)} - \mathbf{D}\mathbf{s}^{(t+1)}) \\ \boldsymbol{\mu}_2^{(t+1)} &= \boldsymbol{\mu}_2^{(t)} + \sigma_2(\mathbf{z}^{(t+1)} - \mathbf{H}\mathbf{x}^{(t+1)}) \end{aligned} \quad (48)$$

Finally the proposed algorithm named as CSIM minimization via Augmented Lagrangian Method (CSIM-ALM), is given in Algorithm 1. There are some points to be noticed. First of all we can use the method of FISTA [24] to accelerate the rate of convergence of the iterative reconstruction of \mathbf{s} using (43). This way the proposed algorithm converges within the first few iterations. Of course this step may be discarded by performing more iterations of the algorithm instead, to achieve similar reconstruction quality. Another remark is that we use a variable (adaptive) regularizing parameter α_1 according to SpARSA [26].

V. SIMULATION RESULTS

A. Experiment 1

In this part, we conduct an experiment to show the performance of the proposed quality assessment criterion compared to some popular criteria, namely MSE, SSIM and FSIM. Consider $\mathbf{x} \in \mathbb{R}^N$ is the reference image signal and $\mathbf{y} \in \mathbb{R}^N$ denotes the noisy observed image, i.e., $\mathbf{y} = \mathbf{x} + \mathbf{n}$ where $\mathbf{n} \in \mathbb{R}^N$ denotes the noise signal which has Gaussian distribution with zero mean and variance σ_n^2 , $\mathbf{n} \sim \mathcal{N}(0, \sigma_n^2)$. Suppose that the image is divided into small patches of size $\sqrt{n} \times \sqrt{n}$. The problem is to find a linear denoising filter $\mathbf{h}_j \in \mathbb{R}^m (m \leq n)$ whose convolution with the j th patch of the image denoted by $\mathbf{y}_j \in \mathbb{R}^n$ gives an estimate of the original patch signal denoted by $\hat{\mathbf{x}}_j$, i.e.

$$\hat{x}_j[i] = \sum_{k=0}^{m-1} h_j[k]y_j[i-k], \quad i = 0, 1, \dots, n-1 \quad (49)$$

After the small patches are denoised, the entire image is then reconstructed by superposition of the recovered patches.

1) *First scenario*: In this case we are given a clean estimate of the original signal \mathbf{x} . This estimate for instance, may be obtained by lowpass (moving average) filtering the noisy image signal in a natural application. But here we simply use the original image signal which is assumed to be known. This is in fact an artificial experiment to assess whether theoretically optimizing the proposed criterion is visually preferred to MSE and SSIM optimization or not. Now if we assume

$y_j[i] = 0$, for $i < 0$, we can restate the equation (49) in algebraic form $\hat{\mathbf{x}}_j = \mathbf{Y}_C\mathbf{h}_j$, where:

$$\mathbf{Y}_C = \begin{pmatrix} y_j[0] & 0 & 0 & \dots & 0 \\ y_j[1] & y_j[0] & 0 & \dots & 0 \\ \vdots & \vdots & \vdots & \dots & \vdots \\ y_j[n-1] & y_j[n-2] & y_j[n-3] & \dots & y_j[n-m] \end{pmatrix} \quad (50)$$

Hence, in this case we have to solve the following optimization problem:

$$\min_{\mathbf{h}_j} f(\mathbf{x}_j, \hat{\mathbf{x}}_j) = f(\mathbf{x}_j, \mathbf{Y}_C\mathbf{h}_j) \quad (51)$$

where f denotes the performance metric we use as the fidelity criterion between the original and the reconstructed signal. If we use CSIM as the fidelity criterion, then the optimal filter \mathbf{h}_j will be obtained by solving the problem below:

$$\mathbf{h}_j^{\text{CSIM}} = \underset{\mathbf{h}_j}{\operatorname{argmin}} \|\mathbf{W}^{\frac{1}{2}}\mathbf{Y}_C\mathbf{h}_j - \mathbf{W}^{\frac{1}{2}}\mathbf{x}_j\|_2^2 = (\mathbf{W}^{\frac{1}{2}}\mathbf{Y}_C)^\dagger \mathbf{W}^{\frac{1}{2}}\mathbf{x}_j \quad (52)$$

We use different approaches to find the optimal denoising filter. Namely we use the MSE, SSIM and the CSIM optimal filters for denoising image patches with different levels of additive noise. The MSE optimal filter is simply obtained by:

$$\mathbf{h}_j^{\text{MSE}} = \underset{\mathbf{h}_j}{\operatorname{argmin}} \|\mathbf{Y}_C\mathbf{h}_j - \mathbf{x}_j\|_2^2 = \mathbf{Y}_C^\dagger \mathbf{x}_j \quad (53)$$

and the optimal filter based on SSIM criterion is achieved by solving the optimization problem below:

$$\mathbf{h}_j^{\text{SSIM}} = \underset{\mathbf{h}_j}{\operatorname{argmax}} \text{SSIM}(\mathbf{x}_j, \mathbf{Y}_C\mathbf{h}_j) \quad (54)$$

This optimization problem is non-convex, but using a linear search method it can be converted to a quasi-convex problem. The similar problem (of course with sparsity constraint) is solved in [57]. Now we use the optimized filters obtained by solving optimization methods introduced above to denoise image patches of size 8×8 distorted with different noise levels. We then compare reconstruction quality of the denoising filters of different orders in terms of PSNR, SSIM and FSIM. Fig 3 shows the performance of the designed FIR filters. For this part the image patches are raster scanned and converted into vectors of size $n = 64$. We also set the parameters of CSIM as $k_2 = n - 1, k_1 = 0.2k_2$. As shown in the figure the proposed metric provides some sort of reconstruction quality which stands between PSNR and SSIM. The denoised patches via CSIM filter have higher PSNR than those having been denoised using the same order SSIM filter. This is approximately the same based on FSIM performance. The difference between these image quality assessment criteria is influenced by the noise level. At high SNR (low noise) the proposed metric is quite similar to MSE or PSNR, whereas at low SNR it behaves much more like SSIM. The FSIM performance also confirms the superiority of the proposed criterion for image denoising compared to MSE and SSIM. This result can also be visually confirmed according to Fig. 1 which shows the denoising results for FIR filters of order $m = 6$. Table I shows the restoration results for entire 256×256 images obtained by

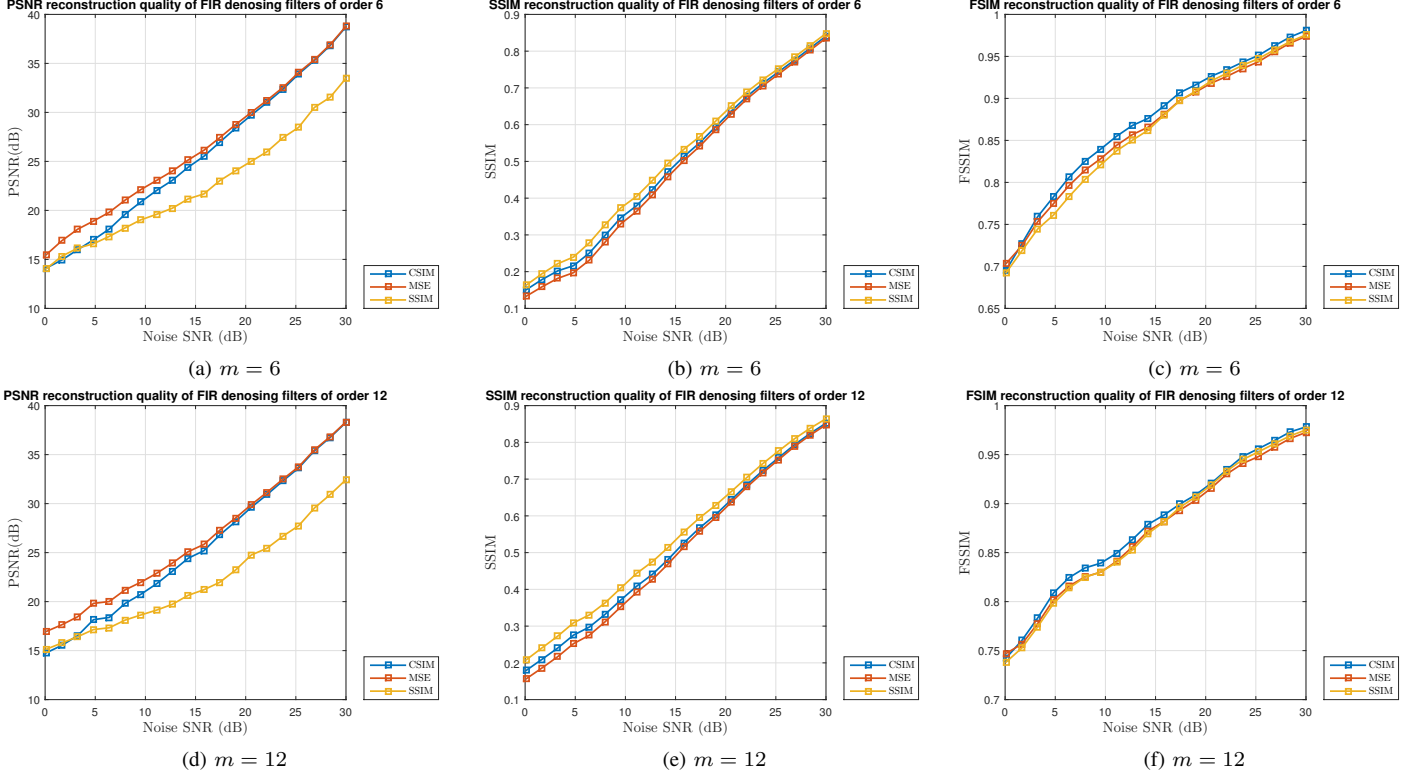


Fig. 3. Quality performance of FIR denoising filters for 8×8 image patches versus noise level. The order of the filter is denoted by m ($k_1 = 12$, $k_2 = 63$)

TABLE II
PERFORMANCE COMPARISON OF THE FIR DENOISING FILTERS OF ORDER m FOR SIMULATIONS IN PART V-A.2 (SNR=1dB)

		$m = 6$			$m = 12$		
		MSE Filter	CSIM Filter	SSIM Filter	MSE Filter	CSIM Filter	SSIM Filter
Peppers	PSNR (dB)	21.64793	21.7143	21.5236	21.49739	21.5663	21.547
	SSIM	0.483457	0.487075	0.48695	0.541758	0.547965	0.545625
	FSIM	0.737972	0.743853	0.74152	0.760147	0.762156	0.759996
	Time (s)	8.671875	8.84375	123.4844	12.90625	12.5	126.6406
Lena	PSNR (dB)	23.4301	23.51699	23.5393	23.27777	23.29914	23.31125
	SSIM	0.509773	0.51945	0.516033	0.554572	0.559539	0.55748
	FSIM	0.76562	0.770744	0.769893	0.779354	0.780314	0.780307
	Time (s)	8.875	8.546875	121.7813	12.73438	12.57813	125.0469
Barbara	PSNR (dB)	22.07703	22.09299	22.06136	21.86944	21.86258	21.80966
	SSIM	0.471681	0.474548	0.47164	0.478401	0.479339	0.473757
	FSIM	0.757897	0.759037	0.755325	0.760586	0.763256	0.756748
	Time (s)	9.09375	8.609375	122.1875	13.15625	12.51563	125.1719
House	PSNR (dB)	23.43906	23.5731	23.52321	24.12948	24.16865	24.10161
	SSIM	0.386421	0.394148	0.390097	0.476552	0.48155	0.479555
	FSIM	0.693577	0.695039	0.694965	0.731814	0.733746	0.732695
	Time (s)	9.09375	8.6875	124.75	13.20313	12.64063	129.3281
Cameraman	PSNR (dB)	22.06733	22.07957	22.05864	22.0714	22.06688	22.10787
	SSIM	0.382708	0.396937	0.39702	0.453836	0.457089	0.454604
	FSIM	0.674499	0.683098	0.681842	0.687971	0.693188	0.689301
	Time (s)	8.921875	8.96875	125.5	13.14063	12.75	123.0781
Couple	PSNR (dB)	22.70483	22.67239	22.69083	22.37438	22.37977	22.38362
	SSIM	0.46712	0.467596	0.470518	0.458069	0.457024	0.454858
	FSIM	0.758213	0.75606	0.758453	0.730827	0.732256	0.728856
	Time (s)	9.25	8.625	124.0313	13.42188	12.29688	125.4844

separately dividing the image into overlapping 8×8 patches and using the FIR denoising filters for local reconstruction. It is clear that for low SNR and the limited number of FIR taps, the proposed method achieves higher reconstruction quality compared to MSE and SSIM methods. Furthermore comparing the complexity or the running time of the denoising process of each algorithm, shows that the optimization of the proposed CSIM criterion, unlike SSIM, is quite as fast and easy as MSE because of its convexity.

2) *Second scenario*: In this scenario the original image signal \mathbf{x} is unknown and unavailable. In fact \mathbf{x} is the vector of spatial samples of a random process $x[i]$ called the image signal, which is assumed to be ergodic and WSS stationary. The clean image signal is then added by a white noise process $n[i]$ whose samples are denoted by \mathbf{n} . The noise process is assumed to be also WSS having Gaussian distribution with zero mean and variance σ_n^2 . The observed noisy image signal \mathbf{y} is thus modelled by the sum of these two random processes. Hence, in this case we are encountered stochastic signals and the problem of finding the equalizer filter, is indeed a linear estimation problem as discussed in [62]. But here we assume stationariness within the spatial domain of each patch. In other words, the small patches of the clean and the noisy image signals denoted by \mathbf{x}_j and \mathbf{y}_j are considered stationary within their corresponding spatial domain. Thus although all the patches are WSS stationary processes of size $n \times 1$, they have different distributions. Hence, we confine ourselves to local patch denoising for estimation of \mathbf{h}_j . The usual fidelity criterion used for estimation is MSE which leads to the so-called Wiener-Hopf equations:

$$\mathbf{h}_j^{\text{MSE}} = \underset{\mathbf{h}_j}{\operatorname{argmin}} \mathbb{E} \left[\left(x_j[i] - \sum_{k=0}^{m-1} h_j[k] y_j[i-k] \right)^2 \right] \quad (55)$$

$$= \mathbf{R}_{y_j, y_j}^{-1} \mathbf{r}_{x_j, y_j}$$

where \mathbf{R}_{y_j, y_j} and \mathbf{r}_{x_j, y_j} denote the auto-correlation matrix and the the vector of cross-correlation components respectively, i.e.,

$$\begin{aligned} \mathbf{R}_{y_j, y_j}[k, l] &= r_{y_j, y_j}[k-l], \quad k, l = 0, \dots, m-1 \\ \mathbf{r}_{x_j, y_j}[k] &= r_{x_j, y_j}[k], \quad k = 0, \dots, m-1 \end{aligned} \quad (56)$$

Now assume the noise process is independent from \mathbf{x} and is distributed homogeneously through the whole image. Using $\mathbf{y}_j = \mathbf{x}_j + \mathbf{n}$, $\mathbf{n} \perp \mathbf{x}_j$ with $\mu_n = 0$ and $c_{n, n}[k] = \sigma_n^2 \delta[k]$, it can be shown that [62]

$$\begin{aligned} c_{x_j, y_j}[k] &= c_{x_j, x_j}[k] = c_{y_j, y_j}[k] - \sigma_n^2 \delta[k] \\ \mu_{x_j} &= \mu_{y_j} \end{aligned} \quad (57)$$

We also have:

$$r_{x_j, y_j}[k] = c_{x_j, y_j}[k] + \mu_{y_j}^2, \quad r_{y_j, y_j}[k] = c_{y_j, y_j}[k] + \mu_{y_j}^2 \quad (58)$$

Instead of the MSE criterion we may use CSIM or SSIM in our estimation problem. If we use the statistical definition of CSIM, the optimization problem for finding the denoising filter

\mathbf{h}_j would be:

$$\mathbf{h}_j^{\text{CSIM}} = \underset{\mathbf{h}_j}{\operatorname{argmin}} k_1 (\mu_{x_j} - \mu_{\hat{x}_j})^2 + k_2 (\sigma_{x_j}^2 + \sigma_{\hat{x}_j}^2 - 2\sigma_{x_j, \hat{x}_j}) \quad (59)$$

where \hat{x}_j is obtained by (49). Now we have the following relations:

$$\mu_{\hat{x}_j} = \mathbb{E} \left[\sum_{k=0}^{m-1} h_j[k] y_j[i-k] \right] = \sum_{k=0}^{m-1} h_j[k] \mu_{y_j} \quad (60)$$

$$\begin{aligned} \sigma_{x_j, \hat{x}_j} &= \mathbb{E} \left[(x_j[i] - \mu_{x_j})(\hat{x}_j[i] - \mu_{\hat{x}_j}) \right] \\ &= \mathbb{E} \left[(x_j[i] - \mu_{x_j}) \left(\sum_{k=0}^{m-1} h_j[k] (y_j[i-k] - \mu_{y_j}) \right) \right] \\ &= \sum_{k=0}^{m-1} h_j[k] c_{x_j, y_j}[k] = \mathbf{h}_j^T \mathbf{c}_{x_j, y_j} \end{aligned} \quad (61)$$

Now if we denote the covariance matrix of \mathbf{y}_j by \mathbf{C}_{y_j, y_j} , the optimization problem (59) is simplified to:

$$\begin{aligned} \underset{\mathbf{h}_j}{\operatorname{argmin}} k_1 (\mu_{x_j} - \mathbf{1}_m^T \mathbf{h}_j \mu_{y_j})^2 + \\ k_2 \left(\sigma_{x_j}^2 + \mathbf{h}_j^T \mathbf{C}_{y_j, y_j} \mathbf{h}_j - 2\mathbf{h}_j^T \mathbf{c}_{x_j, y_j} \right) \end{aligned} \quad (62)$$

This problem is quadratic in terms of \mathbf{h}_j . To solve this we use (57) and we differentiate with respect to \mathbf{h}_j which gives:

$$\begin{aligned} -2k_1 \mu_{y_j}^2 (1 - \mathbf{1}_m^T \mathbf{h}_j) \mathbf{1}_m + \\ 2k_2 (\mathbf{C}_{y_j, y_j} \mathbf{h}_j - \mathbf{c}_{x_j, y_j}) = 0 \end{aligned} \quad (63)$$

Hence,

$$\mathbf{h}_j^{\text{CSIM}} = \left(\mathbf{C}_{y_j, y_j} + \frac{k_1}{k_2} \mu_{y_j}^2 \mathbf{1}_m \mathbf{1}_m^T \right)^{-1} (\mathbf{c}_{x_j, y_j} + \frac{k_1}{k_2} \mu_{y_j}^2 \mathbf{1}_m)$$

To reduce the complexity of calculating the inverse above, having $\mathbf{C}_{y_j, y_j}^{-1}$, we can use matrix inverse lemma.

Now let us turn to SSIM fidelity criterion. The SSIM optimization problem for estimating the optimal equalization filter, tries to maximize the cost function below with respect to \mathbf{h}_j [62]:

$$\left(\frac{2\mu_{y_j}^2 \mathbf{h}_j^T \mathbf{1}_m + C_1}{\mu_{y_j}^2 (1 + \mathbf{h}_j^T \mathbf{1}_m \mathbf{1}_m^T \mathbf{h}_j) + C_1} \right) \left(\frac{2\mathbf{h}_j^T \mathbf{c}_{x_j, y_j} + C_2}{\sigma_{x_j}^2 + \mathbf{h}_j^T \mathbf{C}_{y_j, y_j} \mathbf{h}_j + C_2} \right) \quad (64)$$

This optimization problem is solved via conversion to a quasi-convex format using bi-sectional search method [62].

In practical simulations for denoising image patches, the covariance matrix \mathbf{C}_{y_j, y_j} is empirically obtained using unbiased estimation and we use equation (57) and (58) for the values of σ_{x_j} and μ_{x_j} . The simulation results for denoising with FIR filters are given in table II. It is clear that in the case where the original signals are unknown, the proposed CSIM metric is outperforming the other criteria in terms of estimation quality. It is even faster and performing better than MSE and SSIM in most cases.

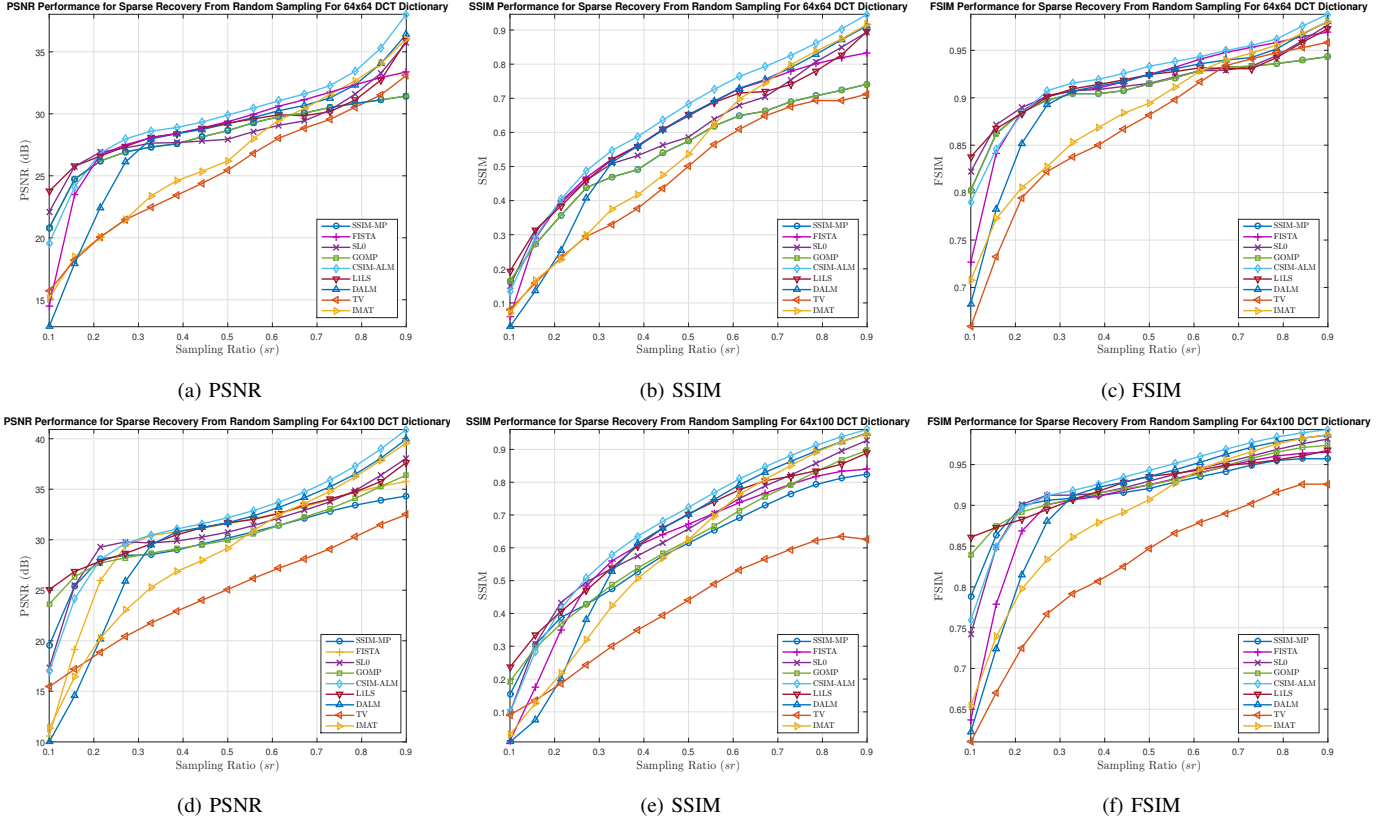


Fig. 4. Quality performance of sparse recovery methods versus the rate of sampling of 64×1 image vectors. In Fig 4a to 4c we have assumed sparse approximation via 64×64 DCT atoms. In Fig 4d to 4f we have used 64×100 DCT atoms.

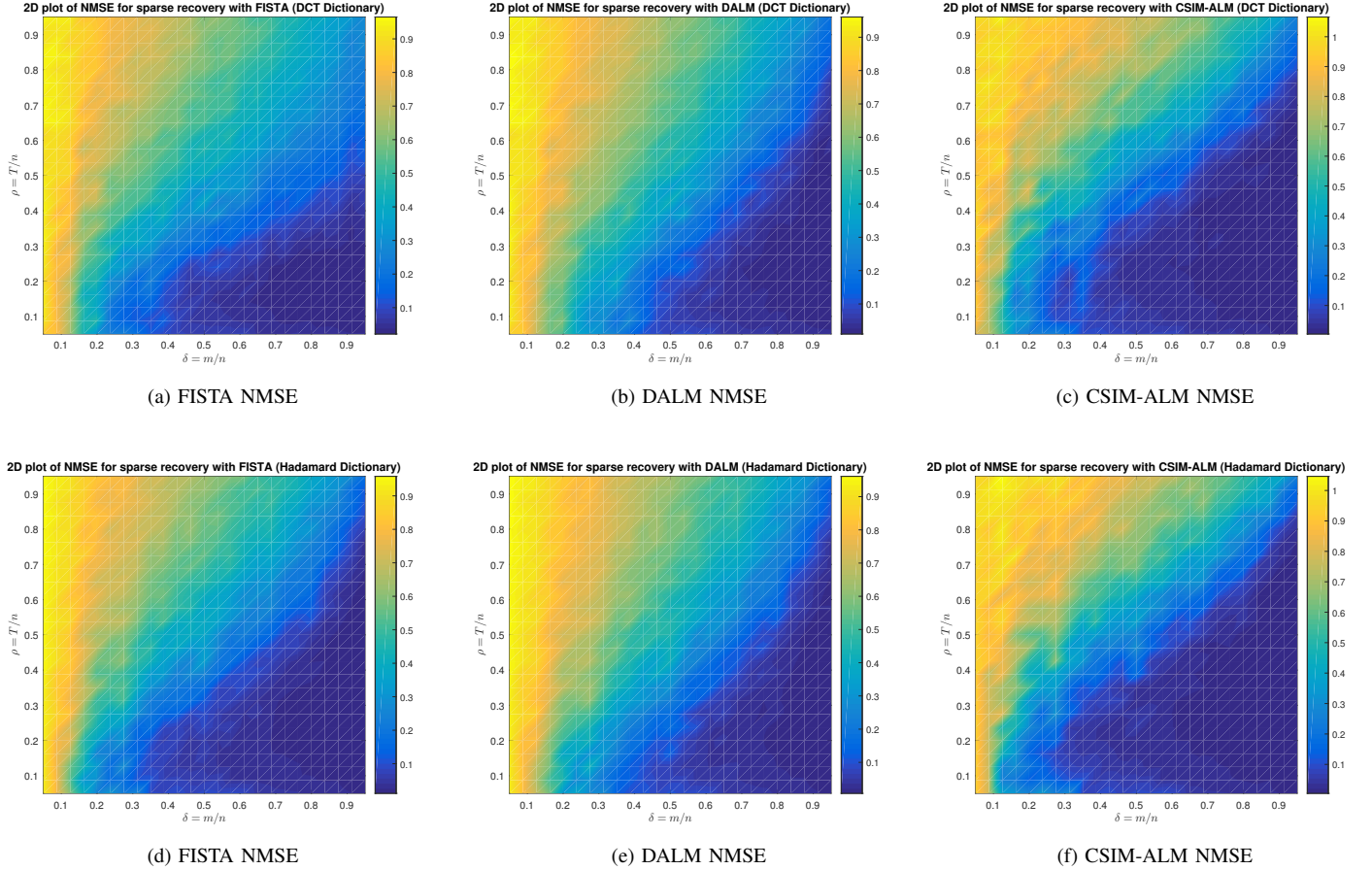


Fig. 5. 2D plot of NMSE versus $\rho = T/m$ and $\delta = m/n(sr)$. We have used 64×64 DCT (7a to 7c) and Walsh-Hadamard (7d to 7f) matrices as \mathbf{D} .

B. Experiment 2

In this experiment we compare the quality performance of the proposed CSIM-ALM method for recovery of missing samples of image patches with some popular sparse recovery algorithms. We use IMAT¹, L1-LS, DALM², TV³ [63], FISTA, SL0⁴, GOMP⁵ and the method in [57] which we call it SSIM-based Matching Pursuit (SSIM-MP).

1) *First scenario*: For simulations of this part, we extract 8×8 patches of sample gray-scale images shown in Fig 2. We then vectorize the patches using raster scanning and select 100 patch vectors of size $n = 64$ denoted by \mathbf{x}_i at random. For each patch, a binary (0,1) random sampling matrix \mathbf{H}_j with size $m_j \times n$ is generated and the observed image signal for each experiment is acquired by $\mathbf{y}_{i,j} = \mathbf{H}_j \mathbf{x}_i$. The locations of 1s in the rows of \mathbf{H}_j (corresponding to m_j sampling indices) are chosen uniformly at random and the sampling ratio of the signal defined as $sr_j = \frac{m_j}{n}$ varies between (0, 1). We use complete (64×64) and over-complete DCT (64×100) dictionaries for reconstruction and we assume sparse representation on the basis of the DCT atoms. This in fact the case where compressible representation is presumed and the exact sparsity is unknown. Hence, to use matching pursuit methods we consider the image patch signal is 10% sparse. After the sparse recovery of missed samples, we then average over random experiments (random \mathbf{x}_i s and random masks with same m_j) and plot the PSNR, SSIM and FSIM of the reconstruction performance, versus the sampling rate. The parameters for SL0 and TV are set to their defaults. We have edited and accelerated the algorithm of FISTA⁶ by removing unnecessary code lines and setting $\beta = 1.2$ and $\eta = 0.9$. The values of the exponential threshold parameters in IMAT is set to $\alpha = 0.2$ and the value of the initial threshold to $\beta = 0.2 \|\mathbf{D}^T \mathbf{H}^T \mathbf{y}\|_\infty$. The stopping criterion for DALM and L1-LS are set to their defaults meaning that the algorithms stop when the duality gap falls below a certain tolerance. The stopping criterion for the remaining algorithms including IMAT, FISTA, SL0 and CSIM-ALM is set to the maximum iteration count which is 50. The parameters for CSIM-ALM are chosen as $\sigma_1 = 0.5$, $\sigma_2 = 4$, $\eta = 0.9$, $\beta = 1.2$, $k_2 = n - 1 = 63$ and $k_1 = 0.2k_2$. Also similar to FISTA, The value of α_{\min} is set to 10^{-6} . Fig. 4 shows the results of the sparse recovery from random samples. As depicted in these figures, the proposed CSIM-ALM algorithm mostly outperforms the state of the art algorithms for sparse recovery via ℓ_1 -norm minimization specifically at $sr > 0.2$. It mainly provides a better reconstruction quality compared to DALM and TV which commonly use the ADMM technique to solve the ℓ_1 optimization problem. This superiority is specifically more apparent in terms of SSIM performance which is shown in the second columns in Fig. 4. The proposed CSIM-ALM algorithm also outperforms the sparse recovery method SSIM-MP which is based on non-convex SSIM maximization. Fur-

thermore the rate of convergence of CSIM-ALM as shown in Fig. 6 is significantly faster than L1-LS and FISTA which uses the same method of acceleration for updating $\mathbf{s}^{(t)}$. The running time for some of these sparse recovery methods is also compared in Fig. 7. The vertical axis in Fig. 6 is the relative error and the vertical axis in Fig. 7 represents the time each iteration takes in seconds. The horizontal axis in these figures also shows the number of iterations which is set to maximum 70 for all algorithms. Since the initial sparse vector is not determined in this case and we only assume sparsity or more precisely compressibility in presentation of the image patches based on DCT atoms, the relative error is defined as:

$$\text{RelErr}_{i,j} = \frac{\|\mathbf{x}_i - \mathbf{D}\mathbf{s}_{i,j}\|}{\|\mathbf{x}_i\|} \quad (65)$$

where $\mathbf{s}_{i,j}$ denotes the sparse vector recovered given the vector of observation samples $\mathbf{y}_{i,j}$. Since SSIM-MP algorithm uses matching pursuit based on a given sparsity, it iterates until all the sparse components of the signal are recovered. Hence, in Fig. 6 and Fig. 7 only 20 iterations of this algorithm (corresponding with assumed sparsity of $\frac{1}{3}$ approximately) are shown and beyond this limit the algorithm usually starts to diverge. Although it may seem that this method which is based on matching pursuit via non-convex SSIM maximization, yields the least reconstruction error within only few iterations, but looking at Fig. 7 it is clear that it takes much longer time than CSIM-ALM to perform only the first iteration of SSIM-MP. In fact SSIM-MP is the most complex algorithm (in our comparison) because of its non-convex optimization behaviour. The least complex algorithms are SL0, DALM and IMAT but they need more iterations to reach stable recovery performance compared to CSIM-ALM. Indeed according to Fig. 6 CSIM-ALM reaches its minimum reconstruction error within roughly 10-15 iterations. This is much less than SL0 for high sr and DALM for low sampling rates.

2) *Second scenario*: In the second scenario, we consider the image signal \mathbf{x}_i is artificially sparse, i.e., it is generated via multiplying a dictionary matrix $\mathbf{D} \in \mathbb{R}^{n \times K}$ by a strictly sparse vector $\mathbf{s}_i \in \mathbb{R}^K$, i.e., $\mathbf{x}_i = \mathbf{D}\mathbf{s}_i$. The T_i non-zero elements of the random sparse signal \mathbf{s}_i are chosen from a Gaussian distribution with $\mathcal{N}(0, 1)$ and the locations of non-zero entries are also chosen uniformly at random. In this scenario we actually compare the reconstruction performance of the proposed algorithm for recovery of T_i -sparse signals with the algorithms introduced in the previous part. We use columns of discrete DCT and Walsh-Hadamard matrices as the atoms of the dictionary \mathbf{D} . Similar to the previous scenario, we investigate the missing sample recovery of the vectors \mathbf{x}_i by generating a sampling matrix \mathbf{H}_j as discussed before. Fig. 5 depicts the 2D plot of Normalized Mean Square Error (NMSE) versus the sparsity $\rho = T_i/m_j$ and the undersampling $\delta = m_j/n$ (or sr_j) ratios. This plot shows the reconstruction NMSE in a 25×25 grid where $\rho, \delta \in (0.05, \dots, 0.95)$. The NMSE in this case where the initial sparse vector is known, is defined as:

$$\text{NMSE}_{i,j} = \frac{\|\mathbf{s}_i - \mathbf{s}_{i,j}\|}{\|\mathbf{s}_i\|} \quad (66)$$

where like before, $\mathbf{s}_{i,j}$ denotes the recovered sparse vector

¹<http://ee.sharif.edu/~imat/>

²<https://people.eecs.berkeley.edu/~yang/software/l1benchmark/>

³<http://www.caam.rice.edu/~optimization/L1/TVL3/>

⁴<http://ee.sharif.edu/~SLzero/>

⁵<http://islab.snu.ac.kr/paper/gOMP.zip>

⁶<https://people.eecs.berkeley.edu/~yang/software/l1benchmark/>

given the observation $\mathbf{x}_{i,j}$. This plot is quite similar to the Phase-Transition Curve (PTC) [64], but here instead of the successful recovery rate, we have plotted the NMSE in two dimensions. Furthermore, we have used DCT and Walsh-Hadamard transform instead of the random projection (Gaussian) matrix which is normally used in the PTC diagram. In Fig. 5, the bluer the mesh color, the lower the NMSE is and as the value of NMSE rises (poor recovery) the color tends to yellow. In this experiment we consider recovery performance of strict sparse signals. The large area of the blue region indicates that the algorithm is more capable of recovering a sparse vector under different circumstances. It is actually proportional to the performance of the algorithm and as it is clear from Fig. 5, the proposed CSIM-ALM algorithm is more efficiently dealing with the signal reconstruction problem compared to FISTA and DALM for recovery of strict sparse signals via DCT and Walsh-Hadamard dictionaries.

VI. CONCLUSION

In this paper, a new performance metric for image quality assessment is introduced which is a modified convex version of SSIM and is called CSIM. This metric like MSE, is well suited for mathematical manipulations and like SSIM, has perceptual meanings. The proposed fidelity metric is used for solving the missing sample recovery problem based on sparse representation of the image patches. This sparse recovery method can subsequently be applied in the sparse coding step in a dictionary learning method which in turn may be used in image inpainting and restoration. In addition, an iterative ADMM-based algorithm is proposed to solve the optimization problem obtained from incorporating the new fidelity metric. The convexity of the optimization problem leads to an efficient iterative convergent algorithm. Simulation results show the efficiency of the suggested new performance metric as well as the superiority of the proposed iterative algorithm over counterpart methods for missing sample recovery of images.

REFERENCES

- [1] Y. Wang, P. Stoica, J. Li, and T. L. Marzetta, "Nonparametric spectral analysis with missing data via the EM algorithm," *Digital Signal Processing*, vol. 15, no. 4, pp. 192–206, 2005.
- [2] L. Stankovic, M. Dakovic, and S. Vujovic, "Adaptive variable step algorithm for missing samples recovery in sparse signals," *IET Signal Processing*, vol. 8, no. 3, pp. 246–256, 2014.
- [3] P. Stoica, J. Li, and J. Ling, "Missing data recovery via a nonparametric iterative adaptive approach," *IEEE Signal Process. Lett.*, vol. 16, no. 4, pp. 241–244, 2009.
- [4] A. Adler, V. Emiya, M. G. Jafari, M. Elad, R. Gribonval, and M. D. Plumbley, "Audio inpainting," *IEEE Tran. Acoustic, Speech, and Language Processing*, vol. 20, no. 3, pp. 922–932, 2012.
- [5] O. G. Guleryuz, "Nonlinear approximation based image recovery using adaptive sparse reconstructions and iterated denoising-part II: Adaptive algorithms," *IEEE Tran. Image Processing*, vol. 15, no. 3, pp. 555–571, 2006.
- [6] C. Guillemot, and O. L. Muer, "Image Inpainting: Overview and Recent Advances" *IEEE Signal Processing Magazine*, vol. 31, no. 1, pp. 127–144, 2014.
- [7] D. Guo, Z. Liu, X. Qu, L. Huang, Y. Yao, and M. T. Sun, "Sparsity-based online missing data recovery using overcomplete dictionary," *IEEE Sensors Journal*, vol. 12, no. 7, pp. 2485–2495, 2012.
- [8] F. Li, and T. Zeng, "A universal variational framework for sparsity-based image inpainting," *IEEE Tran. Image Processing*, vol. 23, no. 10, pp. 4242–4254, 2014.
- [9] D. L. Donoho, "Compressed sensing," *IEEE Trans. Inf. Theory*, vol. 52, no. 4, pp. 1289–1306, 2006.
- [10] E. J. Candes, and T. Tao, "Near-optimal signal recovery from random projections: universal encoding strategies?," *IEEE Trans. Inf. Theory*, vol. 52, no. 12, pp. 5406–5425, 2006.
- [11] F. Marvasti, et al., "A unified approach to sparse signal processing," *EURASIP Journal on Advances in Signal Processing*, vol. 44, 2012.
- [12] S. Mallat and Z. Zhang, "Matching pursuits with time-frequency dictionaries," *IEEE Trans. on Signal Proc.*, vol. 41, no. 12, pp. 3397–3415, 1993.
- [13] J. A. Tropp, and A. C. Gilbert, "Signal recovery from random measurements via orthogonal matching pursuit," *IEEE Trans. Inf. Theory*, vol. 53, no. 12, pp. 5655–5666, 2007.
- [14] D. Needell, and R. Vershynin, "Uniform uncertainty principle and signal recovery via regularized orthogonal matching pursuit," *Found. Comput. Math.*, vol. 9, no. 3, pp. 317–334, 2009.
- [15] D. Needell, and J. A. Tropp, "CoSaMP: iterative signal recovery from incomplete and inaccurate samples," *Appl. Comput. Harmon. Anal.*, vol. 26, no. 3, pp. 301–321, 2009.
- [16] J. Wang, S. Kwon, and B. Shim, "Generalized orthogonal matching pursuit," *IEEE Trans. on Signal Proc.*, vol. 60, no. 12, pp. 6202–6216, 2012.
- [17] T. Blumensath, and M. E. Davies, "Iterative thresholding for sparse approximations," *Journal of Fourier Analysis and Applications*, vol. 14, no. 5, pp. 629–654, 2008.
- [18] S. Zahedpour, S. Feizi, A. Amini, and F. Marvasti, "Impulsive noise cancellation based on soft decision and recursion," *IEEE Trans. on Instrumentation and Measurement*, vol. 11, no. 52, 2003.
- [19] M. Azghani and F. Marvasti, "Iterative methods for random sampling and compressed sensing recovery," *Sampling Theory and Applications, Proceedings of 50th International Conference on EURASIP*, 2013.
- [20] A. Esmaili, E. Asadi, and F. Marvasti, "Iterative Null-space Projection Method with Adaptive Thresholding in Sparse Signal Recovery and Matrix Completion," *arXiv preprint*, arXiv:1610.00287, 2016.
- [21] G. H. Mohimani, M. Babaie-Zadeh, and C. Jutten, "A fast approach for overcomplete sparse decomposition based on smoothed ℓ_0 norm," *IEEE Trans. on Signal Proc.*, vol. 57, no. 1, pp. 289–301, January 2009.
- [22] S. S. Chen, D. L. Donoho, and M. A. Saunders, "Atomic decomposition by basis pursuit," *SIAM Journal on Scientific Computing*, vol. 20, no. 1, pp. 33–61, 1999.
- [23] I. Duabeche, M. Defrise, and C. De Mol, "An iterative thresholding algorithm for linear inverse problems with a sparsity constraint," *Commun. Pure Appl. Math.*, vol. 57, no. 11, pp. 1413–1457, 2004.
- [24] A. Beck, and M. Teboulle, "A fast iterative shrinkage-thresholding algorithm for linear inverse problems," *SIAM. Journal. Imaging Sciences*, vol. 2, no. 1, pp. 183–202, 2009.
- [25] S. J. Kim, K. Koh, M. Lustig, S. Boyd, and D. Gorinevsky, "An interior-point method for large-scale-regularized least squares," *IEEE journal of selected topics in signal processing*, vol. 1, no. 4, pp. 606–617, 2007.
- [26] S. J. Wright, R. D. Nowak, and M. A. T. Figureido, "Sparse reconstruction by separable approximation," *IEEE Trans. on Signal Proc.*, vol. 57, no. 7, pp. 2479–2493, 2009.
- [27] J. Yang, and Y. Zhang, "Alternating direction algorithms for ℓ_1 -problems in compressive sensing," *SIAM. J. Sci. Comput.*, vol. 33, no. 1, pp. 250–278, 2011.
- [28] H. Zayyani, M. Babaie-zadeh, and C. Jutten, "An iterative Bayesian algorithm for Sparse Component Analysis in presence of noise," *IEEE Trans. on Signal Proc.*, vol. 57, no. 11, pp. 4378–4390, 2009.
- [29] D. Wipf, and B. D. Rao, "Sparse Bayesian Learning for basis selection," *IEEE Trans. on Signal Proc.*, vol. 52, no. 8, pp. 2153–2164, 2004.
- [30] S. Ji, Y. Xue, and L. Carin, "Bayesian Compressive Sensing," *IEEE Trans. on Signal Proc.*, vol. 56, no. 6, pp. 2346–2356, June 2008.
- [31] R. Chartrand, "Exact reconstruction of sparse signals via nonconvex minimization," *IEEE Signal Process. Letters*, vol. 14, no. 10, pp. 707–710, 2007.
- [32] Z. Zhang, Y. Xu, J. Yang, X. Li, and D. Zhang, "A survey of sparse representation: algorithms and applications," *IEEE Access*, vol. 3, pp. 490–530, 2015.
- [33] Z. Wang, A. C. Bovik, H. R. Sheikh, and E. P. Simoncelli, "Image quality assessment: From error visibility to structural similarity," *IEEE Trans. Image Processing*, vol. 13, no. 4, pp. 600–611, 2004.
- [34] S. Talebi, and F. Marvasti, "A novel method based on sampling theory to recover block losses for JPEG compressed images" *ICASSP, Istanbul*, 2000.
- [35] H. Hosseini, A. Goli, N. B. Marvasti, M. Azghani, and F. Marvasti, "On Image Block Loss Restoration Using the Sparsity Pattern as Side Information" *arXiv preprint arXiv:1401.5966*, 2014.

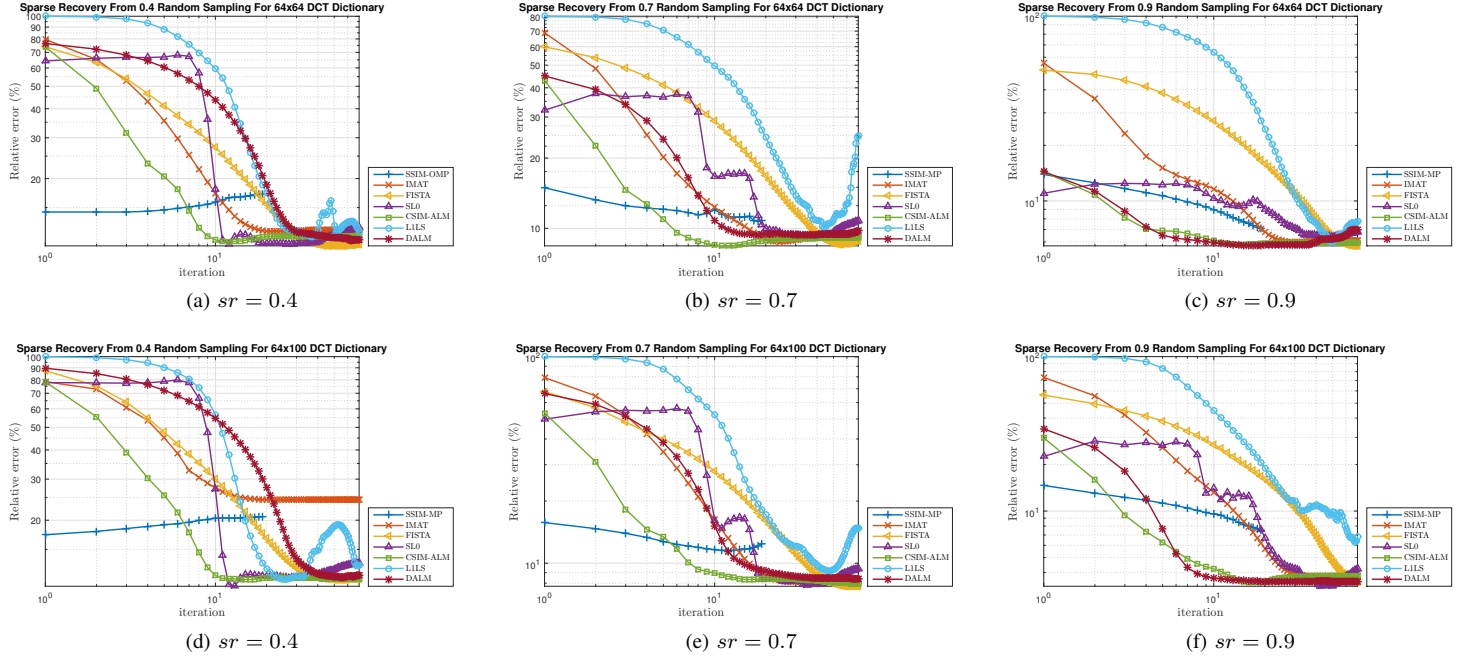


Fig. 6. Relative reconstruction error versus the number of iterations for sparse approximation via 64×64 (6a to 6c) and 64×100 (6d to 6f) DCT atoms.

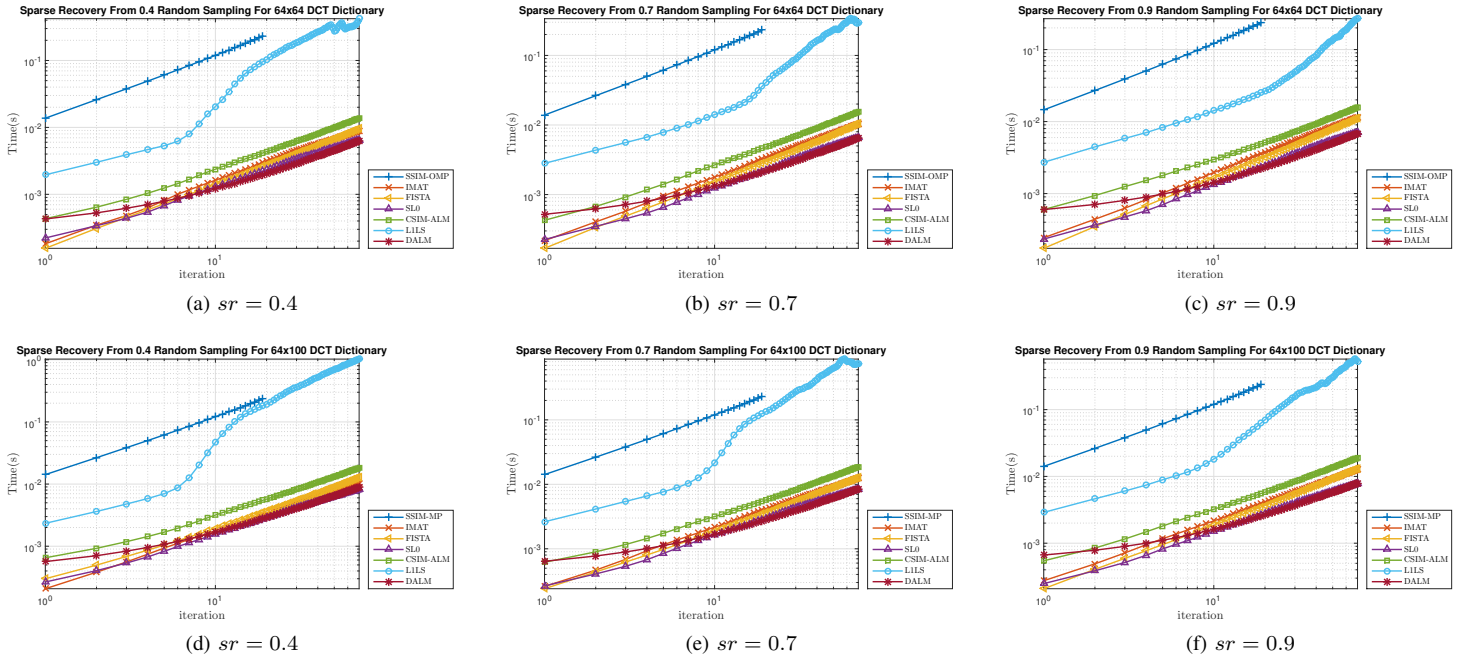


Fig. 7. Running time versus the number of iterations for sparse approximation via 64×64 (7a to 7c) and 64×100 (7d to 7f) DCT atoms.

- [36] M. Bertalmio, G. Sapiro, V. Caselles, and C. Ballester Image inpainting in *Proceedings of the 21th Annual Conference on Computer Graphics and Interactive Techniques*, 2000.
- [37] V. Caselles, G. Sapiro, C. Ballester, M. Bertalmio, and J. Verder, Filling-in by joint interpolation of vector fields and grey levels *IEEE Trans. Image Process.*, vol. 10, pp. 1200–1211, 2011.
- [38] T. Chan, and J. Shen, Non texture inpainting by curvature-driven diffusion *J. Visual Commun. Image Representation*, vol. 12, no. 4, pp. 436–449, 2001.
- [39] M. Bertalmio, A. Bertozzi, and G. Sapiro, Navier-Stokes, fluid dynamics, and image and video inpainting in *Proc. IEEE Int. Conf. on Comp. Vision and Pattern Recog.*, Hawaii, 2001.
- [40] V. Casellas Exemplar-based Image Inpainting and Applications *SIAM News*, 2011.
- [41] A. Criminisi, P. Perez, and K. Toyama, Region Filling and Object Removal by Exemplar-based Image Inpainting *IEEE Transaction on Image Processing*, vol. 13, no. 9, pp. 1200–1212, 2004.
- [42] C. Barnes, E. Shechtman, A. Finkelstein, and D.B. Goldman, Patchmatch: A randomized correspondence algorithm for structural image editing *ACM Transactions on Graphics*, vol. 28, no. 3, 2009.
- [43] B. Wohlberg, “Inpainting by joint optimization of linear combinations of exemplars,” *IEEE Signal Process. Letters*, vol. 18, no. 1, pp. 75–78, 2011.
- [44] M. Elad, J.L. Starck, P. Querre, and D.L. Donoho, Simultaneous cartoon

- and texture image inpainting using morphological component analysis (MCA) *Applied and Computational Harmonic Analysis*, vol. 19, no. 3, pp. 340–358, 2005.
- [45] J. M. Fadili, J. L. Starck, and F. Murtagh, Inpainting and zooming using sparse representations *The Computer Journal, Oxford Journals*, vol. 52, no. 1, pp. 64–79, 2007.
 - [46] M. Aharon, M. Elad, and A. Bruckstein K-SVD: An algorithm for designing overcomplete dictionaries for sparse representation. *IEEE Transactions on Signal Processing*, vol. 54, no. 11, pp. 4311–4322, 2006.
 - [47] J. Mairal, M. Elad, and G. Sapiro Sparse representation for color image restoration *IEEE Transactions on Image Processing*, vol. 17, no. 1, pp. 53, 2008.
 - [48] D. Brunet, E. R. Vrsnay, and Z. Wang, On the Mathematical Properties of the Structural Similarity Index *IEEE Transactions on Image Processing*, vol. 21, no. 4, pp. 1488–1499, 2012.
 - [49] L. Zhang, L. Zhang, X. Mou, and D. Zhang, “FSIM: A Feature Similarity Index for Image Quality Assessment,” *IEEE Tran. Image Processing*, vol. 20, no. 8, pp. 2378–2386, 2011.
 - [50] H. R. Sheikh, and A. C. Bovik, “Image information and image quality,” *IEEE Tran. Image Processing*, vol. 15, pp. 430–444, 2006.
 - [51] Z. Wang, E. P. Simoncelli, and A. C. Bovik, “Multi-scale structural similarity for image quality assessment,” *IEEE Asilomar Conf. on Signals, Systems and Computers*, Nov 2003.
 - [52] T. O. Aydin, R. Mantiuk, K. Myszkowski, and H. P. Seidel, “Dynamic range independent image quality assessment,” *ACM. Trans. Graph.*, vol. 27, pp. 1–10, Aug 2008.
 - [53] H. Yeganeh, and Z. Wang, “Object quality assessment of tone-mapped images,” *IEEE Trans. Image Processing*, vol. 22, pp. 657–667, 2013.
 - [54] P. Mohammadi, A. Ebrahimi-Moghadam, and S. Shirani, “Subjective and Objective Quality Assessment of Image: A Survey,” *Majlesi Journal of Electrical Engineering*, vol. 9, no. 1, pp. 55–83, 2014.
 - [55] D. L. Donoho, “De-noising by soft-thresholding,” *IEEE Trans. Inf. Theory*, vol. 41, no. 3, pp. 613–627, 1995.
 - [56] K., Bredies, and D. A., Lorenz “Linear convergence of iterative soft-thresholding,” *Journal of Fourier Analysis and Applications*, 14(5-6), pp. 813–837, 2008.
 - [57] T. Ogawa, and M. Haseyama, “Image inpainting based on sparse representations with a perceptual metric,” *EURASIP Journal on Advances in Signal Processing*, vol. 1, pp. 1–26, 2013.
 - [58] D. P. Bertsekas, “Constrained optimization and Lagrange multiplier methods,” *Academic press*, 2014.
 - [59] S. Boyd, N. Parikh, E. Chu, B. Peleato, and J. Eckstein, “Distributed optimization and statistical learning via the alternating direction method of multipliers,” *Foundations and Trends in Machine Learning*, vol. 3, no. 1, pp.1–122, 2011.
 - [60] W. W. Hager, “Updating the inverse of a matrix,” *SIAM review*, vol. 31, no. 2, pp. 221–239, 1989.
 - [61] K. Lange, “Optimization” *Springer*, New York (2004)
 - [62] S. S. Channappayya, A. C. Bovik, C. Caramanis, and R. W. Heath, “Design of linear equalizers optimized for the structural similarity index,” *IEEE transactions on image processing*, vol. 17, no. 6, pp. 857–872, 2008.
 - [63] C. Li, W. Yin, H. Jiang, and Y. Zhang, “An efficient augmented Lagrangian method with applications to total variation minimization,” *Computational Optimization and Applications*, vol. 56, no. 3, pp. 507–530, 2013.
 - [64] D. L. Donoho, A. Maleki, and A. Montanari, Message-passing algorithms for compressed sensing, *Proc. Nat. Acad. Sci.*, vol. 106, no. 45, pp. 18 914–18 919, 2009.
 - [65] H. Weyl, Das asymptotische Verteilungsgesetz der Eigenwerte linearer partieller Differentialgleichungen (mlt einer Anwendung auf die Theorie der Hohlraumstrahlung),” *Math. Ann.* vol. 71, pp. 441–479, 1912.